Brain connectivity during different sleep stages using EEG and NIRS

by

Rajani Khanal

Submitted to the College of Science and Engineering in partial fulfilment of the requirements for the degree of Master of Engineering (Biomedical) at Flinders University - Adelaide Australia

Supervisor : Dr. Sherry Randhawa

Co-supervisor: Hanieh Bakhshayesh

27/05/2019

Declaration

I certify that this work does not incorporate without acknowledgment any material previously submitted for a degree or diploma in any university; and that to the best of my knowledge and belief it does not contain any material previously published or written by another person except where due reference is made in the text.

Rajani Khanal

27/05/2019

Acknowledgement

I am extremely thankful for the continuous guidance from my supervisors Dr. Sherry Randhawa and Hanieh Bakhshayesh throughout this project. They have been very patient and considerate about all the aspects of this research work and in absence of their support and motivation, the completion of this project wouldn't be realised. My sincere gratitude goes to A/ Professor Kenneth Pope, and Azinsadat Janani, Flinders University, for their technical advice and suggestions for the betterment of this research work.

My special remembrance to the staff at Adelaide Institute for Sleep Health for their co-ordination and support.

Finally, I thank god, for making me capable of facing the challenges and being my ultimate talisman.

Abstract

Brain connectivity is gaining significant attention at present given its scope to unveil brain mechanisms and functions. Sleep, where brain undergoes cycles of distinct behaviours, is one of the complexities in neuroscience where several brain processes occur together. EEG is a commonly used modality in measuring brain electrophysiological signals and is known for a good temporal resolution. Near Infrared Spectroscopy (NIRS), however, is an emerging modality in neuroscience providing a good deal of information about cerebral hemodynamic with better spatial resolution than EEG. A combination of these two modalities can help reveal underlying neurophysiological and hemodynamic activities in complex brain behaviour such as sleep.

The present study aims to measure brain connectivity during whole night sleep based on combined hemodynamic and electrophysiological signals and see if the measure can aid in differentiating sleep stages. In doing so, whole night sleep and NIRS data were obtained form 5 healthy volunteers and two common measures of connectivity: transfer entropy and cross-correlation were applied. The focus of the study is particularly on effective connectivity, in terms of prefrontal hemodynamic, and EEG covering frontal, central and occipital brain regions. Statistical validity and reproducibility of the findings were analysed with ANOVA and permutation test.

Connectivity measures revealed causal influence to be directed from prefrontal to posterior brain regions. Also, the highest brain connectivity was found during NREM1 sleep with a fair decrease in the measure as sleep progresses to further stages. Significant difference in connectivity was found in the prefrontal region between wake and NREM1, NMREM2 and REM sleep stages. Hemodynamic changes during the different sleep stages could be better understood with these findings.

Our findings suggest that brain connectivity measure using NIRS and EEG carry the potential to aid in sleep staging along with information about hemodynamic changes throughout sleep that can help better understand the regulation and functions of sleep. Nevertheless, further research with similar approaches, could help accurately estimate sleep stage and understand full picture of brain mechanisms for sleep regulation.

***Keywords**: connectivity, sleep stages, hemodynamic, EEG, NIRS, oxyhemoglobin, de-oxyhemoglobin*

List of abbreviations

AASM: American Academy of Sleep Medicine

EEG: Electroencephalography

NIRS: Near Infrared Spectroscopy

PSG: Polysomnography

ANOVA: Analysis of variance

HBO: Oxyhemoglobin

HHB: De-oxyhemoglobin

EOG: Electrooculogram

EMG: Electromyogram

MVAR: Multivariate autoregressive

DTF: Directed Transfer Function

PDC: Partial directed coherence

GC: Granger causality

PLV: Phase locking value

KL: Kullback–Leibler

EMA: Exponential moving average

CBI: Correlation based index

Table of contents

List of figures

List of tables

Chapter 1 : Introduction and objectives

1.1Introduction

Humans spend almost a third of their life sleeping which has its role in reenergising body cells, clearing wastes, developing memory and cognition, as well as in regulating mood and hunger [1]. As complex as it is, several mysteries related to regulation and functions of sleep remain unexplored yet. Moreover, the prevalence and increasing incidences of sleep disorders [2] require the physiology and pathophysiology of sleep to be well understood. Sleep staging and architecture are two primary tools that help understand the phenomenon of sleep, and polysomnography (PSG) is the most commonly used technique at present to classify sleep stages and diagnose sleep disorders [3]. PSG, however, is a tedious tool requiring time and effort and sleep scoring is done manually by a person. Moreover, it doesn't provide information about brain mechanisms during sleep. Hence, researches have been directed towards finding alternative to PSG in the form of automatic sleep scoring schemes as well as measures that could more precisely estimate integration of brain functions throughout sleep [4, 5].

Brain connectivity is a technique that establishes links between brain areas, that could be structurally connected or located distant apart. Measures of brain connectivity provide quantified relation between such brain regions and help identify the patterns of communication, signal or information flow and functional integration during complexes processes [6**].**

Activities in brain are characteristically rendered by the electrophysiological signal arising from neuronal conductance while hemodynamic signals related to blood flow, oxygenation and physiological signals arising from other body parts such as respiration and heart rate, imply direct or indirect influences on brain activities [7]. At present, most of the connectivity measures are used

in combination with electrophysiological signals [8]. We hypothesize that connectivity measures that include two or more of these signals could infer wholesome knowledge regarding cerebral coordination as well as provide an advantage of extracting information about dual parameters during complex processes like sleep. Hence, we choose to apply connectivity measures to two kinds of brain signals: EEG signal, which is the brain electrical activity measured form the scalp, and NIRS signal, which is the measure of hemodynamic signals in brain cortex.

Sole application of EEG cannot infer hemodynamic changes while that of single NIRS device alone cannot infer causal connections because of the close-ended nature of NIRS channels, i.e., small distance between receiver and transmitter. Hence, this research aims at tracing the connectivity between EEG channels and NIRS channels distributed in the frontal, central, and occipital brain regions. As such, connectivity during different stages of sleep will be analysed and in a broader sense, the research will examine if sleep staging can be simplified using NIRS or if it can act as a supplementary to EEG in PSG for sleep staging.

Various measures of connectivity have been published so far with their own advantages and disadvantages [9]. Since the research aims to find out patterns of information flow and connections in brain during different sleep stages involving two different modalities, we choose two measures for our research: transfer entropy and cross-correlation. Cross-correlation measure can find out the functional connectivity [10] while transfer entropy can also detect causal influences [11]. Hence, these measures when applied to EEG and NIRS signals during different sleep stages could render important information about functional and causal relationships in brain. These relationships can be expected to vary throughout sleep given the scoring of sleep into different states each with its peculiar characteristics.

The report presents the research work carried out with sleep, EEG and NIRS signal in relation to brain connectivity, and is organised in to 5 important sections. The 1st part where we currently are, provides with the research, objectives, overview and executive summary. The second part deals with relevant literature, including necessary background knowledge on brain connectivity, connectivity measures, sleep and previous works in the related field. The 3rd part is the methodologies which serially describes the flow of this project run from sourcing the data to application of connectivity measures and data analysis. The 4th and 5th part of this report present the results and discussions over them.

1.2 Objectives

1.2.1 General objectives

The major direction of this research work is to evaluate brain connectivity during the different sleep stages with the help of NIRS and EEG signal. If there exists substantial difference in connectivity across different stages, this fact could be used to develop a system for automatic sleep staging. The hypothesis is that the neuronal activities during sleep are accompanied by hemodynamic changes so that a measure of functional relation and direction of causal influence between these processes helps to better understand the regulation of sleep.

1.2.2 Specific objectives

1. To quantify connectivity as a measure of transfer entropy between EEG signal and oxyhemoglobin (HBO), and de-oxyhemoglobin (HHB) signal
2. To measure cross-correlation between NIRS signal in the prefrontal region
3. To assess changes in hemodynamic activities in the prefrontal region during different sleep stages.

Chapter 2 : Literature review

2.1 Brain connectivity

Brain delivers signals required to sustain life and perform functions ranging from simple senso-motor to complex cognitive tasks. It does so via a complex network of regions that may be linked in structure, or spatially remote, but connected to one other in a particular manner. The relation between such brain regions is known as brain connectivity [12]. Brain connectivity is an essential tool in assessing the brain processes, the flow of information within brain, associated neuronal areas, and changed conditions during pathology.

Connectivity can be established via ways of anatomical links, statistical dependencies, or via causal relationships. This gives rise to three different modes of connectivity as introduced by Friston [13].

2.1.1 Anatomical connectivity

Anatomical connectivity arises due to physical or structural connections among brain regions. Microscale anatomical connectivity comprise of neuronal synapses and their strengths, which at present, are mostly traced by means of invasive studies. At higher scale, anatomical connectivity would refer to fibre-linked, widely distributed brain regions, as understood from various imaging techniques [14]. White matter tracts in cerebral cortex are the predominant anatomical connections on brain [15].

2.1.2 Functional connectivity

Functional connectivity refers to the underlying synchrony between two brain regions without taking into account the cause of connection or casual influence of one region over the other [16]. It measures synchrony among different brain regions that may be spatially segregated. It accounts

to the activation or deactivation of functionally integrated brain areas to process and execute a common function.

2.1.3 Effective connectivity

Definition by Norbert Wiener [17] suggests effective connectivity to exist from time series X to Y if the future value of Y can be better predicted by knowing the past values of X rather than past values of Y alone. It thus considers the influence one brain region has on the other when executing a function and that may be direct or indirect [18]. Moreover, the influence of one brain region may call for activation or deactivation of another brain region in order to execute a task. Thus, effective connectivity is a notion of directed causal influence and is asymmetric. For instance, a signal released at one part of cerebral cortex may trigger or deactivate signal release at another brain region.

The relation between the different types of connectivity is interesting. The anatomically attached brain regions might not have any functional relation while two distant regions may be integrated functionally and causally.

2.1.4 Brain networks

Brain networks are the mathematical illustrations of connections among different brain regions, normally deployed in the form of nodes connected by links. The nodes ideally represent regions of connections while the links are the modes of connection, i.e., structural, or functional or causal connections. Thus, networks pictorially dictate brain connectivity [19].

The links in a brain network denote different properties based on their type. For instance, binary links are the ones which give information about existence of any connection. Weighted links give additional information about the strength of such connections in terms of density, size or

correlation. Another form of link is the directed or undirected form. In representing anatomical and effective connectivity, directed links are often used as they can trace the direction of connection among the nodes [20].

The figure below shows the brain network derived from structural, functional and effective connectivity datasets. Structural connectivity datasets are obtained from tract tracing and diffusion/ structural MRI, functional datasets from fMRI, EEG and MEG while effective connectivity datasets are derived from causal relations in functional connectivity data. Functional networks are normally undirected as the dataset contains information about functionally connected brain regions without considering the degree of influence, while effective brain networks provide directional information with regards to the influence one region has on the other. Anatomical connectivity, however, could result directed or undirected networks restating the fact that anatomical connectivity can be persistent in micro or macro level throughout the brain [19, 20].

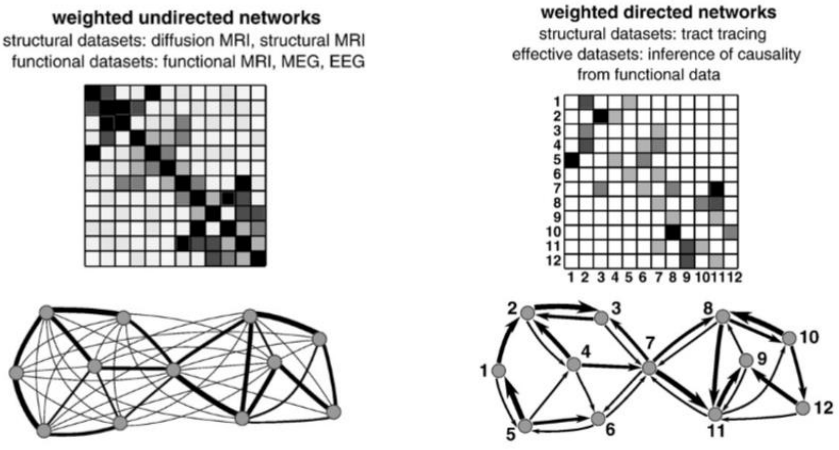

Figure 1: Brain networks derived from connectivity datasets [20]

2.2 Brain connectivity measures

Brain connectivity can be quantified using mathematical relations and models. At present, with the growing interest towards understanding brain processes, numerous brain connectivity measures have been published [9]. These measures of connectivity can be categorized based on whether they measure functional or effective connectivity, based on their method they apply such as linear or non-linear analysis, model or model free analysis, and time or frequency domain analysis. This section details commonly known connectivity measures based on four different methods.

2.2.1 Classical linear methods

2.2.1.1 Cross-correlation

Cross-correlation is a signal processing tool which identifies how two signals are identical in terms of relative displacement [21]. The cross-correlation between two linear time series: x(n) with its average $\bar{x}$ and standard deviation σ_x; and y(n) with mean $\bar{y}$ and standard deviation $\sigma_{y,}$ each of length N is given by:

$$Cor = \frac{1}{N}\sum_{n=1}^{N}\frac{1}{\sigma_x\sigma_{y,}}(x(n) - \bar{x})(y(n) - \bar{y}) \qquad 2\text{-}1$$

Cross-correlation is normally used to analyse time series signals and their synchronization as it cannot infer causal relations [22]. Its use has been profound in studying resting state as well as task-based brain conditions and functional connectivity [23, 24]. Its value is between 0 and 1 where 0 shows non-existence of synchrony and 1 shows maximal functional relation between the two signals under evaluation.

2.1.2. Coherence

Coherence refers to the statistical derivation of relation accompanying two linear signals in the frequency domain. It is also called magnitude-squared coherence. Unlike cross correlation, this measure can estimate causal relation between signals if they are characterised by a linear transfer function. For two signals x(t) and y(t), the coherence is given as [25]:

$$C_{xy}(f)=\frac{|Gxy(f)|^2}{Gxx(f)Gyy(f)} \qquad 1\text{-}2$$

Where,

G_{xy} is cross-spectrum between the two signals,

G_{xx} the x(t) auto-spectrum,

G_{yy} the y(t) auto spectrum.

2.2.2 Model based methods

2.2.2.1 Granger causality (GC)

Wiener's definition of effective connectivity [6] was formalized for mathematical implementation by Granger by applying linear regression models. Granger suggested that reduction in the variance of prediction error in an autoregressive model for a time series Y by including the past values of time series X rather than just using past values of Y indicates the existence of effective connectivity from series X to Y [26].

The bivariate auto regressive model representation is [26]:

$$X(t)= \sum_{j=1}^{p} A_{11}(j)X(t-j) + \sum_{j=1}^{p} A_{12}(j)\,Y(t-j) + e_1(t) \qquad 2\text{-}2$$

$$Y(t) = \sum_{j=1}^{p} A_{22}(j)\, Y(t-j) + \sum_{j=1}^{p} A_{21}(j)\, X(t-j) + e_2(t) \qquad 2\text{-}3$$

Where e(t) is the prediction error.

The connectivity between these series can then be measured by incorporating the variation in prediction error. For instance, in signal Y, if variance in e_2 (t2) is less than that in e_2 (t1) after incorporating signal X in the prediction, the signal X has casual influence on Y and vice-versa.

Connectivity measures using GC have been carried in extensive areas including resting state brain, [27], tasks requiring cognition and perception, [28] hemodynamic convolution, [29] and in anaesthesia. However, Granger Causality comes with the need to have a predefined model to compare with a bivariate autoregressive model limiting its use in non-linear, multivariate signal. Extensions to GC in the form of conditional GC (CGC) and multivariate GC (MVGC) to apply in multivariate signals, and functional GC (FGC) to apply in function domain signals have also been studied to meet the need of multiple applicability [30, 31, 32].

There are two other measures that analyse the multivariate data in frequency domain using Grange Causality [33, 34]:

2.2.2.2 Directed Transfer Function (DTF)

Multivariate autoregressive (MVAR) models make inferences about interregional dependencies among datasets by computing the past influence of one variable on the other. DTF is a MVAR model-based method which at a frequency f, uses transfer function matrix H (f) to compute causal relation between two channels. The DTF value lies between 0 and 1 [34].

For two channels i and j, the DTF gives a ratio of input to channel i from j to input from all other channels as [34]

$$DTF^2_{j\to i}(f) = \frac{|H_{IJ}(f)|^2}{\sum_{m=1}^{k}|H_{im}(f)|^2} \quad 2\text{-}4$$

2.2.2.3 Partial Directed Coherence (PDC)

PDC is also a GC derived, MVAR model-based method which differs from DFT in the sense that it gives a ratio of output from channel (j) to (i), to all other output from the former channel [35].

Consider a Fourier transform matrix A (f) with the j^{th} column as $a_j(f)$. Then the PDC is given by:

$$P_{ij}(f) = \frac{A_{ij}(f)}{\sqrt{a_j^*(f)\, a_j(f)}} \quad 2\text{-}5$$

2.2.3 Phase based method

2.2.3.1 Phase locking value (PLV)

PLV is a functional connectivity measure based on the assumption that the difference in instantaneous phase of two signals from functionally connected brain regions remains fairly constant [36]. In order to obtain instantaneous phase, narrowband filtering for a number of times becomes a crucial step before applying PLV. Thereafter for two signals that have undergone N number of filtering trials, the phase difference (θ) between the two signals for n^{th} trial at time point t is given by [36]:

$$\text{PLV}=\frac{1}{N}\left|\sum_{n=1}^{N} e^{i\theta(t,n)}\right| \quad 2\text{-}6$$

PLV thus focuses on the phase relationship of signals under evaluation and gives a result or either 1 or 0, corresponding to peak phase synchrony and absence of synchrony respectively.

2.2.4 Information theory-based method

Information theory was originally founded by Claud Shannon which measures information contained in a variable as its entropy, called Shannon entropy [37]. Measure of Shannon entropy of a specific variable reduces the uncertainty related to that variable.

Shannon entropy [37]:

$$H = \sum_x p(x) I(x) = - \sum_x p(x) log_a(p(x)) \qquad 2\text{-}7$$

Where,

I(x) is the information contained during an event, expressed with probability of occurrence of event x, as:

I(x) = -log (p(x))

For two dependent systems x and y, Shannon entropy is given by:

$$H_1 = - \sum_{x,y} p(x,y) log(p(x,y)) \qquad 2\text{-}8$$

Where, p(x, y) is now the joint probability of events x and y occurring together.

If the systems are independent of each other, the expression is:

$$H_2 = - \sum_{x,y} p(x,y) log(p(x)p(y)) \qquad 2\text{-}9$$

The difference between H_1 and H_2 gives the system output considering the two system are independent of each other, despite their actual relationship. This output is quantity of mutual information shared between the two processes. This information, however, is not enough to predict future values of the system based on present values [38].

2.2.4.1 Kullback–Leibler (KL) divergence

KL divergence is the deviation of a probability distribution from the reference probability distribution. It is thus not a statistic method but based on mere distribution given by expectation operation of difference in log of actual probability distribution and the reference probability distribution [39]:

$$D_{KL}(p|q) = \sum_{i=1}^{N} p(x_i).(\log p(x_i) - \log q(x_i)) \qquad 2\text{-}10$$

Which can also be written as:

$$D_{KL}(p|q) = \sum_{i=1}^{N} p(x_i).(\log \frac{p(x_i)}{q(x_i)}) \qquad 2\text{-}11$$

Where,

p refers to probability distribution in the actual data to be analysed,

q is the reference probability distribution.

A 0 KL divergence indicates two identical probability distributions [40]. It has been used in studying brain anatomy and structural connectivity [41].

2.2.4.2 Transfer entropy (TE)

TE is a measure of shared or transferred information between time series processes. Transfer entropy gives effective prediction of future values from present instances.

Transfer entropy can be derived by defining entropy rate for the time series data. The entropy rate is in fact, the quantity of further information needed to predict future values of a time series data [42].

Considering two systems x and y, entropy rate defined to predict the value of preceding observation in time series of one of these systems is given by:

$$h_1 = - \sum_{x_{n+1}} p(x_{n+1}, x_n, y_n) log_a \, p\,(x_{n+1}|x_n, y_n) \qquad 2\text{-}12$$

From definition of probability and conditional probability [32]

For x and y to be independent:

$p(y|x)=p(y)$

or,

$p(x, y)= p(y|x)p(x)=p(y)p(x)$

Considering that the value x_{n+1} is not dependent on the present value of y_n, we can define another entropy rate given by:

$$h_2 = - \sum_{x_{n+1}} p(x_{n+1}, x_n, y_n) log_a \, p\,(x_{n+1}|x_n) \qquad 2\text{-}13$$

Then the transfer entropy form system y to x is given by the difference between h2 and h1 as:

T.E from y to x:

$$h_2 - h_1 = \sum_{x_{n+1}, x_n y_n} p(x_{n+1}, x_n, y_n) log_a \, \frac{p(x_{n+1}|x_n,\ y_n)}{p(x_{n+1}|x_n)} \qquad 2\text{-}14$$

Since tranfer entropy is assymetric measure,

T.E from x to y:

$$h1 - h2 = \sum_{y_{n+1}, x_n, y_n} p(y_{n+1}, x_n, y_n) log_a \, \frac{p(y_{n+1}|x_n,\ y_n)}{p(y_{n+1}|y_n)} \qquad 2\text{-}15$$

Now, extending equation (i) from definition of conditional probabilities [43],

We get the TE as:

$$\text{T.E } (y \rightarrow x): \sum_{x_{n+1},x_n,y_n} p(x_{n+1},x_n,y_n)\ log_a \frac{p(x_{n+1},x_n,\ y_n).p(x_n)}{p(x_n,y_n).p(x_{n+1},x_n)} \qquad 2\text{-}16$$

$$\text{T.E } (x \rightarrow y): \sum_{y_{n+1},x_n,y_n} p(y_{n+1},x_n,y_n)\ log_a \frac{p(y_{n+1},x_n,\ y_n).p(y_n)}{p(x_n,y_n).p(y_{n+1},y_n)} \qquad 2\text{-}18$$

Thus, TE output is such that a system Y provides certain digit of prediction to system X, and vice-versa [44]. The range of output varies from 0 to infinity.

According to Weiner, causal dependencies exist between X and Y if the predictability of values of Y is well resolved by applying the information from past of X rather than just relying on the past information of signal Y itself [17]. As such, reducing the uncertainty of one variable (Shannon entropy) and improving the predictability of another signal (effective connectivity) forms a basis of information based effective connectivity measure [45]. Connectivity measures based on information theory avoid the need to know about neural interactions beforehand and development of a respective model.

2.2.4.2.1 Application of transfer entropy for brain connectivity measure

The applicability of transfer entropy in finding effective connectivity as found by Schreiber (2000) has been successively followed by implementations in neurologic studies [45].

Vakorin et al. (2000) explored functional connectivity in EEG data using transfer entropy. They have used it together with partial least square analysis of independent components in the data series [46]. Palus et al. (2001) applied transfer entropy to dig into synchronization events in epileptic patients using EEG data [47]. Sabesan et al., (2009) also analysed the significance of TE in measuring directed information flow in epileptic research [48]. Similarly, Garofalo et al., (2009) recommended TE as a good method to trace functional connectivity in existing neural networks

where data is obtained from multiples sites after they used the same technique for in-vitro networks [49]. Furthermore, Vicente et al., (2011) put an insight into the usefulness of TE to trace the effective connectivity using electro physiological signals from MEG. They found that transfer entropy is an efficient tool to assess effective connectivity in non-linear, model-free and multivariate data, along with those involving volume conductions such as EEG [50].

More recently, Faes et al., (2015) evaluated the sleep EEG rhythms together with elements of changing heart rate using TE and GC. They applied the measures to each pair between high frequency component of heart rate variability and EEG waves (alpha, beta, theta, sigma and delta power bands). The findings comprised of networks representing brain-heart interactions that predominantly consisted of links from heart rate variability to EEG waveforms during whole night sleep. They also suggested that non-linear dynamics and non-parametric TE measure is significant in revealing peculiar structure of information transferred between heart and brain during whole night sleep [51].

2.2.4.2.2 Pros and cons of using transfer entropy for brain connectivity

The fact that transfer entropy avoids the need to develop a pre-model for neural interactions, makes it a suitable measurement tool where the actual process among brain regions is unknown. Moreover, its applicability to non-linear and multivariate data has been quite promising which broadens the scope of its implementation since most of the neuroscientific data is in these forms [38]. Specifically, in effective connectivity measure, the potential of transfer entropy in tracing out causal dependencies despite significant delays in signal transmission, as reported by Swadlow et al., (2012) is a strong advantage [52].

Despite these advantages, the usefulness of transfer entropy is limited by the fact that its output is a number that dictates the quantity of information shared between two brain areas. However, it

does not infer any solution regarding how the system operates. Moreover, the information obtained from transfer entropy does not lead to model development with actual variable involved in the system, such as amplitude or power of signals and state of activation or deactivation [38].

This work intends to find the connectivity between EEG and NIRS during different sleep stages using the transfer entropy method whose output is in the form of bits of information carried by different channels.

2.3 Modalities for characterizing brain activity

At present, there are several modalities for mapping brain activity during different processes. The modalities can be grouped into two kinds based on the parameter they focus on: modalities characterizing brain electrophysiology and those mapping hemodynamic and metabolic brain responses.

The most common modalities for assessing brain electrophysiology are: Electroencephalography (EEG) and Magneto-encephalogram (MEG). These are both based on the electrical signals developed in the brain by numerous neuronal interactions. EEG applies electrodes on scalp to get a measure of these electrical activities whereas MEG measures magnetic field produced by these electric fields within the brain. One drawback of MEG over EEG is - it requires highly specialized, shielded room to carry out tests to avoid magnetic interferences and hence is not very feasible for all kinds of experiments [53].

There are a number of modalities for measuring brain hemodynamic and metabolic changes. Positron emission tomography (PET) is one of them which involves injecting a radioactive molecule in the blood stream to analyses internal processes and hence not very suitable for whole night sleep studies as the radioactive molecule is absorbed by tissues and organs within an hour.

Moreover, it possesses risks for pregnant women, diabetic patients and infants, limiting its use. [54]. Magnetic Resonance Imaging (MRI) involves exposing the subject in a magnetic field to pick up changes related to blood oxygen level. It is heavy, noisy, requires shielded rooms and thus not suitable for long term studies [55]. Transcranial Doppler sonography is also a cerebral monitoring tool primarily functioning to measure relative cerebral blood velocity. It is not very useful in sleep studies because of its insensitivity to oxygenation changes and cannot provide information about regional blood flow [56]. Near infrared spectroscopy is a tool that can assess local blood flow along with oxygenation changes non-invasively. Its availability in portable form make its use preferential in sleep studies [57].

This research uses EEG and NIRS to trace functional and effective connectivity in brain during different sleep stages. This way, the physiological basis of coupled electrical activities and blood oxygenation changes will be assessed.

2.3.1 Electroencephalography (EEG)

EEG is the electrophysiological recording of waves arising from the neuronal activities in the brain, particularly at post synapsis. It is obtained with the help of electrodes attached at different head locations covering major regions over the cerebral cortex. The difference in voltage between one electrode and another selected as a reference electrode forms an EEG channel. The number of required channels used can vary from 4 to 256 as per the nature and scope of the study [58].

The standard for placing electrodes to obtain EEG signal has been provided by the *International Federation in Electroencephalography and Clinical Neurophysiology* as the popularly known *10-20 electrode placement system* [59].

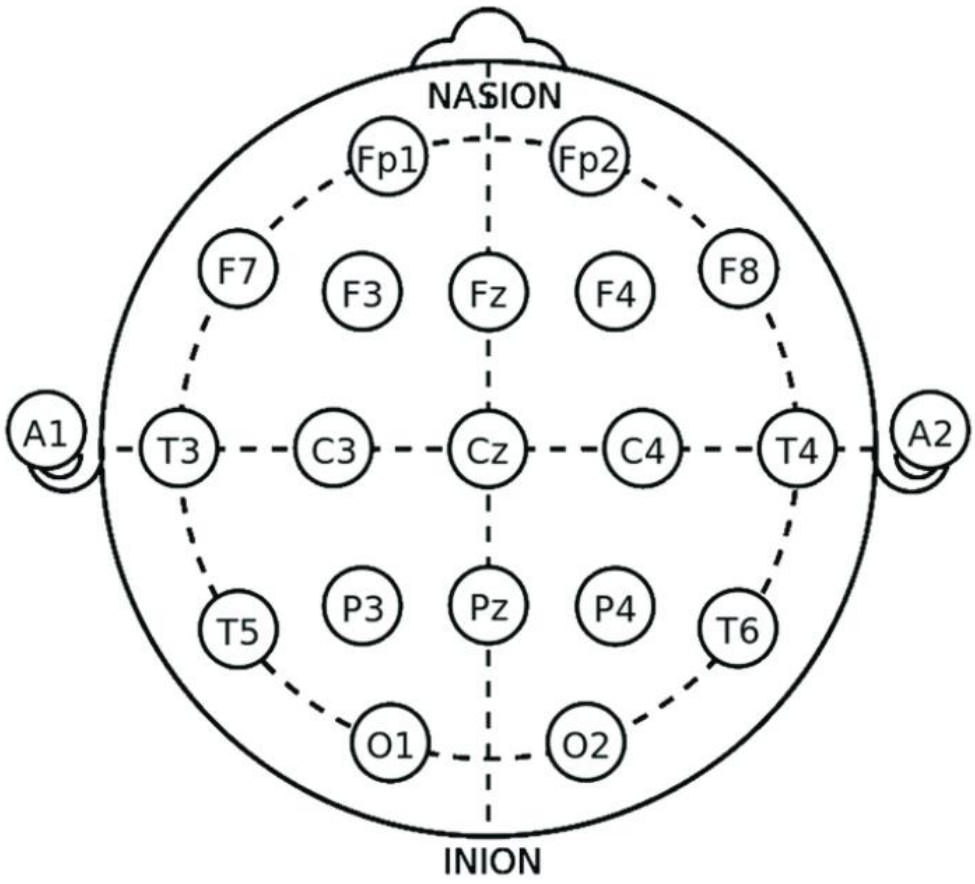

Figure 2: The 10-20 Electrode placement system with 21 channels [59]

2.3.2 Near-infrared spectroscopy (NIRS)

NIRS is an imaging modality which incorporates non-invasive, optical and portable features, and exerts radiations having near-infrared wavelengths (750-2500 nm). It has been used in several medical applications such as pulse oximetry, neuroimaging, blood sugar monitoring etc. The non-invasive and non-ionizing feature, good temporal resolution and cheapness compared to MRI, makes NIRS an emerging technology for hemodynamic studies in sleep medicine [60].

2.3.2.1 Principle

NIRS can find the quantity of light absorbing tissue in the body relying on Beer-Lamberts law. which is given by [60]:

$$OD\ \lambda = Log\frac{I_0}{I} = \varepsilon\lambda.c.L \qquad 2\text{-}17$$

Where,

OD ג is the absorbing medium's optical density,

I_0 is intensity of the light incident,

I is intensity of the light transmitted,

Ɛג is the extinction coefficient at given wavelength

c is the light absorbing substance concentration

L is the path travelled by light within the absorbing medium

λ is the wavelength (nm) used.

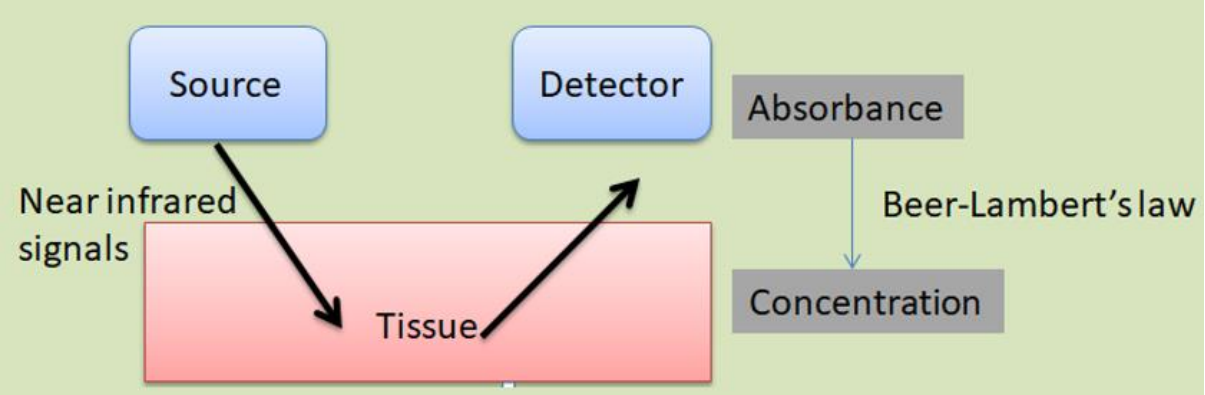

Figure 3: Working principle of NIRS

As shown in figure (3), the NIR light is passed through the source to the tissue where the light is absorbed based on the concentration of absorbing material and the remaining is transmitted back to the detector on the device. Using pre-set Beer-Lambert's algorithm on the absorbing material properties, the concentration is then calculated.

In case of oxyhemoglobin and de-oxyhemoglobin the absorption spectra are distinct in near infrared region as shown in figure (4). As a result, based on their difference in attenuation of incident infrared signals concentration of oxy and de-oxyhemoglobin can be calculated.

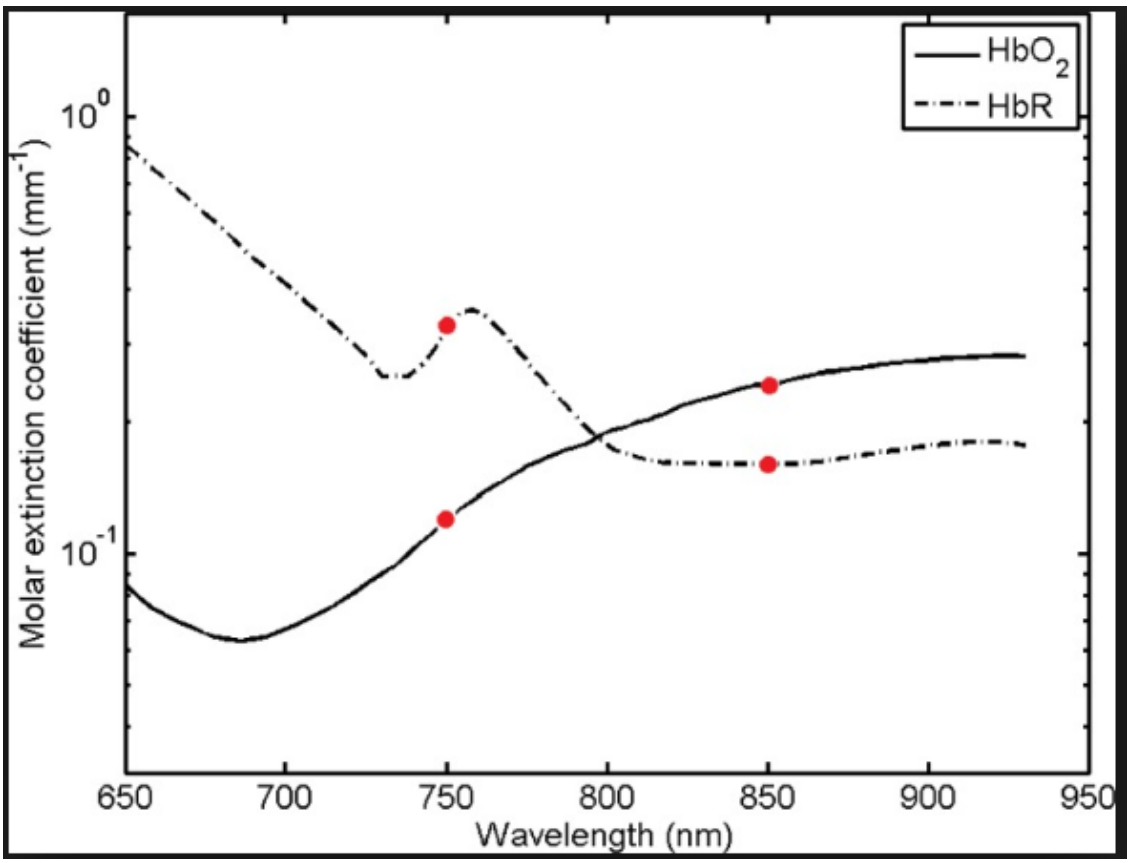

Figure 4: Absorption spectra of oxyhemoglobin (shown as HbO_2) and de-oxyhemoglobin (shown as HbR) in near infrared region [61]

2.3.2.2 NIRS during sleep

The non-invasive and non-ionizing feature, good temporal resolution and cheapness makes NIRS an emerging technology in sleep medicine. During different sleep stages, the neuronal activities are accompanied by alterations in the amount of oxygen bonded haemoglobin [HBO] and oxygen free haemoglobin [HHB] showing oxygen-dependent absorption of near infrared spectrum. Moreover, consumption of 90% of oxygen in a cell is catalysed by an enzyme Cytochrome (Cyt.

Ox). So, a measure of the concentration changes in Cytochrome Ox can give a measure of oxygen concentration changes within a cell as well. Hence changes in oxygen concentration in brain during different sleep stages can be estimated from absorption spectrum and properties of oxidized Cytochrome in the NIR zone.

However, the given Beer Lambert principle is for a non-scattering medium. For an oxygen independent scattering medium like human tissue, the Beer-Lamberts law has been modified as follow [62].

$$OD\ \lambda = \varepsilon\lambda.\ c.\ L.\ B + OD_{R,\lambda} \qquad 18$$

Where,

$OD_{R,\lambda}$ is light intensity loss that is not depended on oxygen concentration due to other elements in the medium that are capable of scattering/absorbing the light.

For a constant $OD_{R,\lambda}$ throughout data collection, the concentration change can be measured from optical density as:

$\Delta c = OD\lambda / \varepsilon\lambda.\ L.\ B$

Hence, hemodynamic variations can be measured using this principle.

2.3.2.3 Portalite

Portalite is a device based on NIRS that is used in cerebral oxygenation measurement. It can be connected to a computer via Bluetooth for up to 100m. It comes with pre-developed software oxysoft which allows easy data collection and analysis. It allows sampling at the rate of upto 50 Hz. It is small and portable making its use desirable in sleep studies [63].

Portalite has three channels formed by combining 3 transmitters (LEDs) and 1 receiver/detector. Each transmitter transmits two wavelengths: 760 and 850 nm. A combination of one receiver and one transmitter forms an optode and distance between them is called optode distance (30, 35, 40mm). One of the channels can be used to measure absolute oxygenated haemoglobin percentage, and the remaining three channels to measure relative concentrations [63].

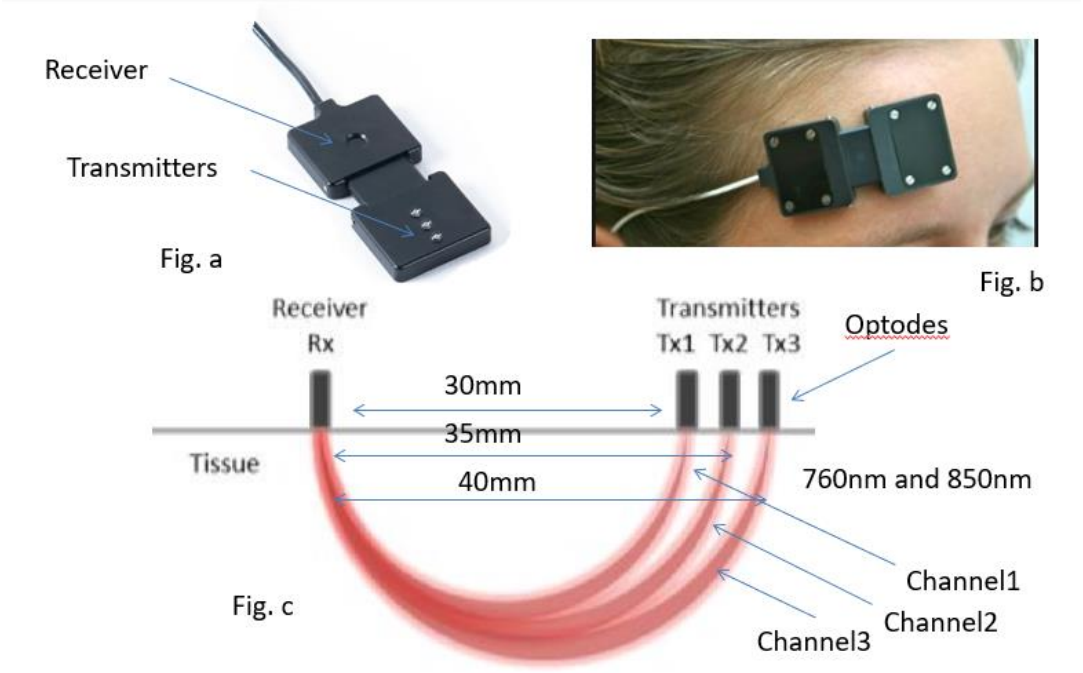

Figure 5: Portalite showing its receiver and transmitters, (b) Placement of Portalite on forehead for data collection, (c) Channels, optodes and optode distance for the Portalite [63].

2.3.2.4 Noise in NIRS

2.3.2.4.1 Types of noise

Abdelnour et al., (2010) suggested three types of the noise accompanying NIRS signal: instrument noise which lie in the high frequency range, motion artefacts and noise caused by physiological signals such as blood flow, respiration and pulsations. [64]. Physiological noise includes that from other body signals like heart beats (1–2 Hz) and blood pressure (about 0.1 Hz) while motion

artefacts arise from body movement of the subject or relative motion of NIRS device on the body, primarily consisting of spikes and ripples [65].

2.3.2.4.2 Method of noise removal

2.3.2.4.2.1 Exponential moving average (EMA)

EMA is a noise removal method similar to the real-time band pass filtering [66]. It is a 1st order infinite impulse response filter that gives different weights to the data in different locations within the sampling window that decrease exponentially. The resulting signal is a difference between short-term S(t) and long-term L(t) moving averages of the signal. If f(t) is the initial signal, the output signal G (t) is a filtered form obtained as [66]:

$$L(t) = \frac{1}{\alpha_L} f(t) + (1 - \frac{1}{\alpha_L}) L(t-1)$$

$$S(t) = \frac{1}{\alpha_L} \sum_{k=0}^{\alpha_s} f(t-k)$$

$$G(t) = S(t) - L(t)$$

Where, α_L is 100 and α_s is 20.

2.3.2.4.2.2 Threshold based method of motion artefact removal

It is a software-based method developed by Fekete et al., (2011) that allows rectification of signal in only the contaminated segments [65]. The method first identifies the affected area as signal spikes and ripples followed by their rectification. Signal spikes are the short, almost instantaneous inflections of the signal soon returning to the baseline value while ripples are prolonged, often long-spanned events. Basically, the magnitude of inflection of spikes and ripple apexes together with the start and end points are computed and then the fluctuations are filtered out leaving only the closest extrema point.

2.3.2.4.2.3 Correlation Based Index method

It is a method based on the inverse relation between two signals under consideration as explained by Cui et al., (2010) [67]. It can be assumed that the extracted signal of oxyhemoglobin (x) and de-oxyhemoglobin (y0) is not pure but also comprises of noise that can produce similar effects on oxy and de-oxyhemoglobin signals (F) as well as some other forms of high frequency, equal intensity noises (N) with constant (α). For the true oxyhemoglobin (x_0) and de-oxyhemoglobin (y_0) signals,

$X = x_0 + \alpha F + N$

$Y = y_0 + F + N$

The method assumes that signal x_0 and y_0 are inversely correlated (maximum -1)

$x_0 = -\beta y_0$

Where, β addresses the amplitude difference between oxy and de-oxyhemoglobin signals.

$F = \frac{1}{\alpha + \beta}(x + \beta y)$

$x_0 = \frac{\beta}{\alpha + \beta}(x - ay)$

The second assumption is that x_0 and Fare negatively correlated (minimum 0). Then, we have,

$\sum_t x^2 + (\beta - \alpha) \sum_t xy - \alpha\beta \sum_t y^2 = 0$

For α=β,

We get,

$\alpha = \sqrt{(\sum x^2) / \sum y^2)}$

=std (x)/ std (y)

Thus, we get,

$$x_0 = \frac{1}{2}(x-\alpha y)$$

$$y_0 = -\frac{1}{\alpha}x_0$$

Based on these derivations, Cui et al., (2010) also suggested that anti-correlated HBO and HHB signals indicate that the signal is fairly free of motion artefacts [67].

2.4 Sleep

Sleep is an everyday recurring phenomenon characterised by reduced sensory and motor activities, movements and reflexes. It forms a cycle with the awake stage in order to maintain the daily body requirements [68]. During sleep, the body's systems like immune, endocrine, muscular, nervous and skeletal are replenished while also strengthening the cognitive and memory functions [69]. A normal person needs to sleep for an average of 8 hours although the fact may vary according to age and health condition of the person. Sleep occurs in various stages forming a sleep cycle. A sleep cycle runs for about 90-110 minutes with each stage contributing about 5-15 minutes [70].

2.4.1 Sleep stages

American Academy of Sleep Medicine (AASM) identifies that there are five distinct stages in a sleep cycle including wakefulness [71]:

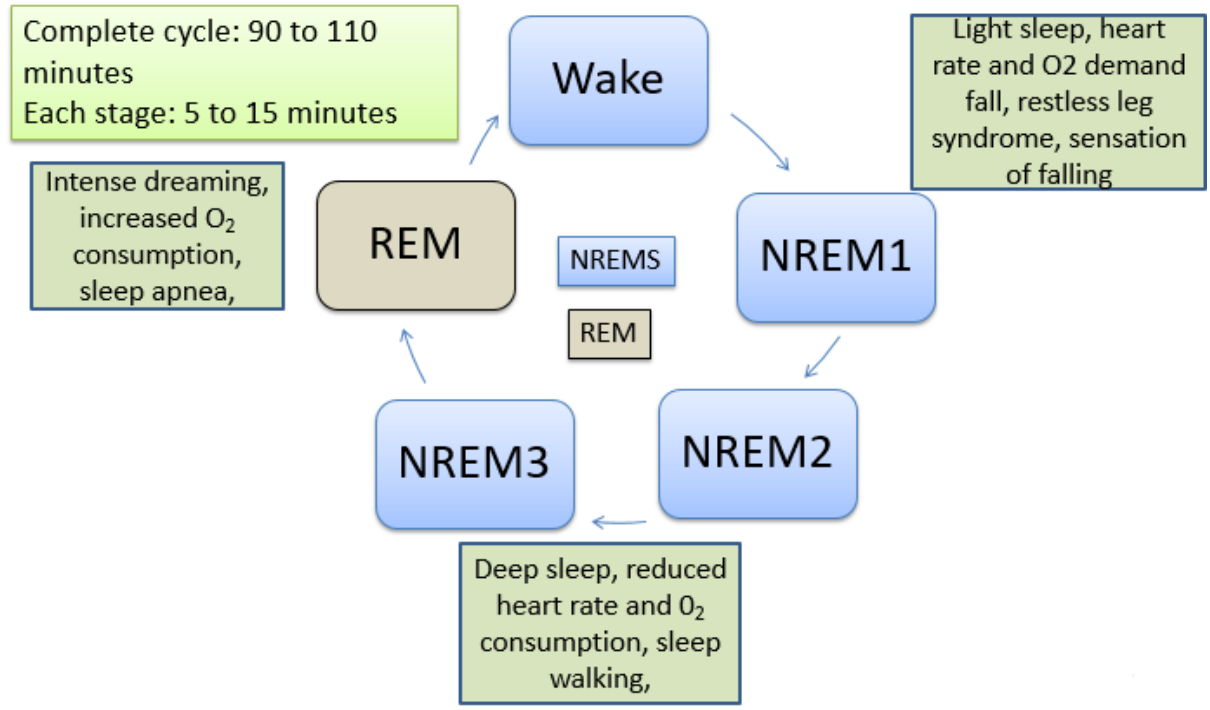

Figure 6: Illustration of sleep stages.

The cycle needs not to be exactly as shown here as a person may wake up before REM or may never enter REM sleep.

Features of the different sleep stages have been discussed below [71, 72]:

The wake stage (W)

It is the time of the day when we are not asleep, aware of the surrounding and consciously interacting with the environment. In an awakened stage, brain and muscle activities are increased. The awakened stage has peculiar alpha waves having mixed frequency and a voltage in the range of 10 to 30 μV in the EEG signal.

Non-Rapid eye movement stage 1 (NREM 1)

In this phase, a person is in light sleep, prone to be awakened quickly. It is characterized by reduced heart rate, slow eye movements, slowed down brain waves and reduced muscular activity. People get sensations of falling or sudden jerks at this stage of sleep. The 1st NREM sleep can be marked as a distinct stage by the appearance of theta waves in EEG which are similar to the alpha ones except that their highest voltage may reach up to 200µV. These waves are also in the mixed frequency range and can be accompanied by slow movements of eyes.

Non-rapid eye movement stage 2 (NREM 2)

In this stage, the person is about to get into deep sleep. The arousal and awakening threshold is higher at this stage than at N1. Brain waves slow down further, heart rate and temperature slightly drop down. NREM stage 2 has the presence of characteristic waves: sleep spindles along with some intermittently occurring K complexes in the EEG signal. As shown in figure 7, K complexes are intermittent, high negative amplitude waves while sleep spindles are higher frequency (12-14 Hz) waves. The slow waves are absent in this stage unlike wake and N1 stages.

Non-Rapid eye movement stage 3 and 4 (NREM 3)

It is the stage of complete, slow wave sleep, where it would be difficult to awaken a person. This is the reason that people with disorders such as parasomnia and sleep walking are difficult at control at this phase. This stage of sleep provides the maximum restoration of body organs and functions. The stage of deep sleep is characterized by instances of slow waveforms for less than half of the epoch. These are the delta waves with a frequency and voltage amplitude of about 2Hz and 75µV.

Stage R: Rapid Eye movement sleep stage

This phase of sleep is featured with rapid movement of eyeballs within closed eyelids. This can be explained by the increased brain activities and neuronal signals during this stage of sleep. The stage is particularly a dreaming stage where the person literally feels that he is in a place that he sees on the concurrent dream. The REM sleep stage has a presence of characteristic sawtooth waves throughout with intermittent, slower delta waves for most of the epoch. During a PSG, this stage shows occasional rapid eye movements in the EOG.

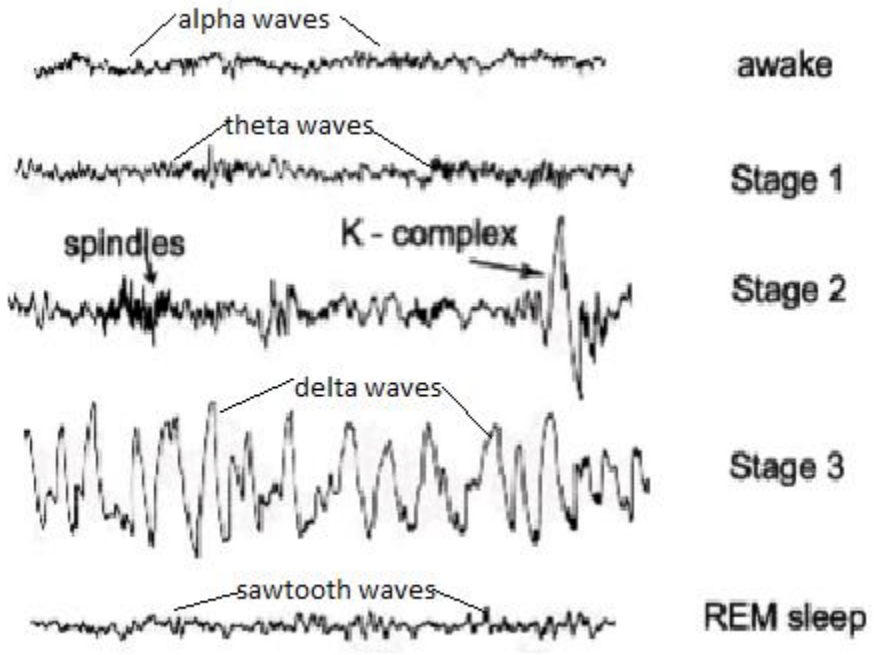

Figure 7: Characteristic EEG waveforms during different sleep stages [72]

2.4.2 Sleep architecture

Sleep architecture refers to the hypnogram plot of continuous sleep stages against time in hours during a whole night study. A sleep architecture reveals that there are normally 5-6 cycles of sleep in a night in an ordinary person. Moreover, the instances of N3 are mostly seen during the early hours of sleep while that of R stages are usually on the later hours of the night as shown in a sleep architecture of a normal person below [73].

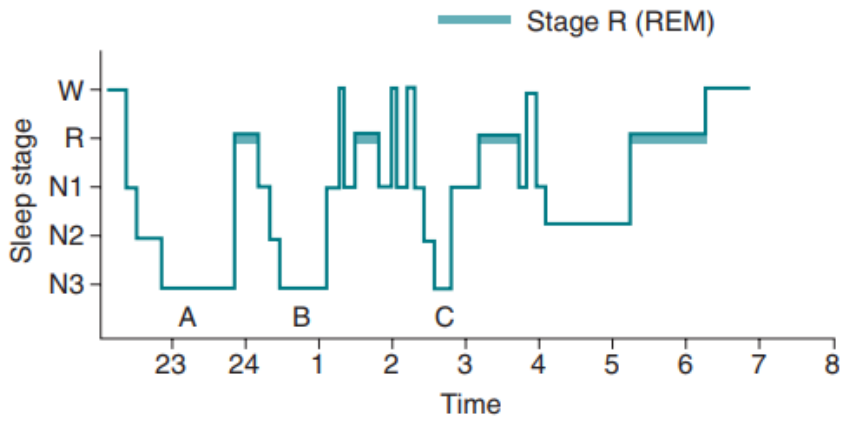

Figure 8: Sleep architecture of a normal person [72]

2.4.3 Sleep disorders

Sleep disorders include the noticed or unnoticed sleep behaviours such as apnoea, sleep walking, parasomnias, bed-wetting, restless leg syndrome, and night terrors. The result is not just a disturbed sleep but also an affected next-day-performance including day-time sleepiness, reduced productivity, etc. Furthermore, the long-term consequences include invasion of diseases such as cardiopulmonary and kidney diseases attributing to physiological disturbances caused by sleep disorders [74].

Sleep disorders not only affect the individual person but in long run it can be noticed that the economic burden created by these disorders is even scarier. According to Hilman et al (2006), in the year 2004 alone, the overall cost associated with sleep disorders was USD 7,494 million which included the direct treatment cost, cost of injuries at workplace, accidents while driving, and loss of efficiency at work; all borne by the sleep disorders in one or other form [75] It is hence, of utmost importance that the diagnosis of sleep disorders be easier, systematic and detailed so that the conditions can be treated on time.

2.4.4 Sleep study

The commonly practiced method of sleep study is an overnight polysomnography (PSG). EEG is one of the vital components in sleep study and is carried out with the help of electrodes placed on the scalp as specified by the *10-20 International system of EEG electrode placement* [59]. Besides EEG, it includes evaluation of the brain (EEG), muscles (EMG), eyes (EOG), and heart signals (ECG), along with the use of pulse oximeters, position sensors, nasal cannula and thermistors, snore sensors, leg motion sensors, respiratory bands and abdominal bands to get the measure of important physiological variables that are needed for sleep scoring [76]. As such the conduction of Polysomnography involves lots of electrodes and wires attached to the subjects/patients that can be messy and not very portable. A full PSG is normally applied in diagnosing persistence of sleep disorders of any form.

Table 1: Location of electrodes and sensors on body and face [71]

Name of Electrode/ sensors	Location	Use

EOG1	1cm out and 1cm up from right eye	Recording of right eye movement
EOG2	1cm out and 1cm down from the left eye	Recording of left eye movement
Chin EMG1	On the chin at which the muscle can be felt beneath the skin when the jaw is clenched	Recording of chin muscle tension
Chin EMG2	Between EMG1 and EMG2	Recording of chin muscle tension
Chin EMG3	On the chin at which the muscle can be felt beneath the skin when the jaw is clenched	Recording of chin muscle tension
ECG1(-)	Over the right clavicle	Recording heart signals
ECG2(GND)	Over the left clavicle	Recording heart signals
ECG3(+)	Between the fifth and sixth rib of left side.	Recording heart signals
Thoracic respiratory band	Around the patient's chest	Sleep staging
Abdominal respiratory band	As low as possible around the abdomen	Sleep staging
Nasal cannula and thermocouple	Nostril	Respiratory measurement in Sleep staging

Oximeter	One of the fingers	Recording blood oxygen saturation
Limb motion sensors	Over the bulk of the tibialis anterior muscle	Recording leg movements
Position sensor	Placed together with thoracic respiratory band	Recording body position during sleep
Snore sensor	Over Adam's apple	Recording instances of snore

2.5 Basis for combined use of EEG and NIRS for connectivity measure during sleep

EEG has been commonly used in sleep studies within PSG. NIRS on the other hand, is a new tool in sleep studies. The applicability of NIRS was first reported by Jobsis (1977) who intended to use it as an optical tool to measure the concentration of cytochrome oxidase enzyme in monitoring tissue metabolism [77]. Therafter, NIRS was used in neonatal and adult cerebral oxygenation monitoring [78, 79]. Followed by this, the applicability of NIRS to measure volume of blood in brain, variations in flow rate as well as muscle oxygenation were also studied [80, 81, 82].

Besides, NIRS has been a technique of interest for many neuroimaging researchers given its ability to measure the concentration changes non-invasively [80, 81]. As a result, the usefulness of NIRS has been depicted in evaluating language learning, cognitive functions, and palaeoecological functions [82, 83, 84].

Nasi et al (2011) used the NIRS device in order to record the hemodynamic changes in brain oxygenation during a whole night sleep study. Their study focused on identifying hemodynamic changes during the transition of sleep stage from one to another. They found that spontaneous hemodynamic activity during slow wave sleep (characterised by delta waves in EEG) is greatly

reduced compared to wakefullnes. Furthermore, the research suggests that transition from wakefullness to light sleep is characterised by reduced physiological activity, that from slow wave sleep to light sleep by increased heart rate and vasoconstiction, and from light sleep to REM byincreased sympathetic activity relating to rapid eye movements and intense dreaming, as obtained form the NIRS hemodynamic parameters [85].

Some researchers have directed their focus on using NIRS in monitoring potients with obstrctive sleep apnoea and in charatcerising transitions from sleep to awake stage [86, 87]. These studies suggest that NIRS carries the potential to aid in sleep staging. This fact has further been studied by Münger et al (1998) who found the connection between the different sleep stages and variations in cerebral oxygenation level in healthy infants [88]. Similarly, Onoe et al., (1991), found in a research with monkeys that REM stage is accompanied by distinct hemodynamic changes in the forebrain [89].

Despite these many researches with NIRS, small attention has been paid to the connectivity measure between NIRS data and EEG during the sleep stages. Wallois et al., (2012), used simultaneous measurement of EEG and NIRS in understanding language learning patterns in the brain. They present the fact that synchronisation in brain can result from multiple synaptic or non-synaptic means of communication among neuronal and glial cells revealing that even before synchronisation takes place, there can occur significant hemodynamic changes. These patterns of synchronisation cannot be detected by using only the electrical recordings but rather by getting the simultaneous hemodynamic signals as well. [90].

Roche- Labarbe et al., (2011), found out that there is a correlation between electric discharges and hemodynamic changes in epileptic children by means of simultaneous EEG and NIRS monitoring [91].

Similarly, advantage of acquiring EEG and NIRS simultaneously to understand cognitive behaviour and possible usage in brain computer interfaces have been studied. Interestingly, in a study by Nguyen et al., (2017), it was found that combined EEG and NIRS measurement allowed detection of drowsy state in drivers differentiating it from the conscious awake stage. The direction of the study was to track if combined EEG and NIRS would be an effective tool to detect drowsiness which seemed to be as expected showing changes in hemodynamic levels and beta bands in the EEG during transitions from awake to drowsy states [92].

These studied have provided with a recommendation that simultaneous EEG and NIRS data collection can aid in deriving important conclusions regarding complex brain behaviours during whole night sleep [93, 94].

Chapter 3 : Methodologies

3.1 Ethics

The study involving whole night PSG and NIRS was approved by the Flinders University Social and Behavioural Research Ethics Committee (project number: 8267). The experimental protocol was considered to be in compliance with the *National Statement on Ethical Conduct in Human Research* [95]. The study was carried out at the sleep lab based at Adelaide Institute for Sleep Health, Flinders University. All participants filled and signed a written, consent form before data collection.

3.2 Participants

2 male and 3 female participants (mean age 29.2 years) volunteered for data collection. Potential participants with any prominent sleep disorders were excluded. Prior to study, the experimental protocol was explained to each of them. Each subject also completed the Epworth Sleepiness Scale [96] and Pittsburgh Sleep Quality Index [97] questionnaire form and declared that they had no medical condition of concern.

3.3 Protocol for data acquisition

Upon arrival at the sleep lab, the participants got their anthropometric measurements done which included their height, weight and age followed by the PSG and the Portalite probe set up for data acquisition

3.3.1 PSG data acquisition

Whole night PSG data was acquired using the Grael PSG by Compumedics®. The procedures followed the standard in-lab PSG as per the AASM guidelines [71]. The EEG channels were notch filtered at 50 Hz. Also, HPF and LPF with cut-off at 0.3 Hz and 30 Hz respectively were

implemented for EEG, EOG and ECG signals. The EMG signal was also subjected to HPF and LPF with cut-off at 10 Hz and 100 Hz respectively.

3.3.1.1 Electrodes on head

EEG signals were obtained based on the *10-20 International system of EEG electrode placement* [59] from 6 channels: two frontal (F3-M2, F4-M1), two central (C3-M2, C4-M1), and two occipitals (O1-M2 and O2-M1) with respect to the mastoids on their contralateral side and ground was taken at Cz.

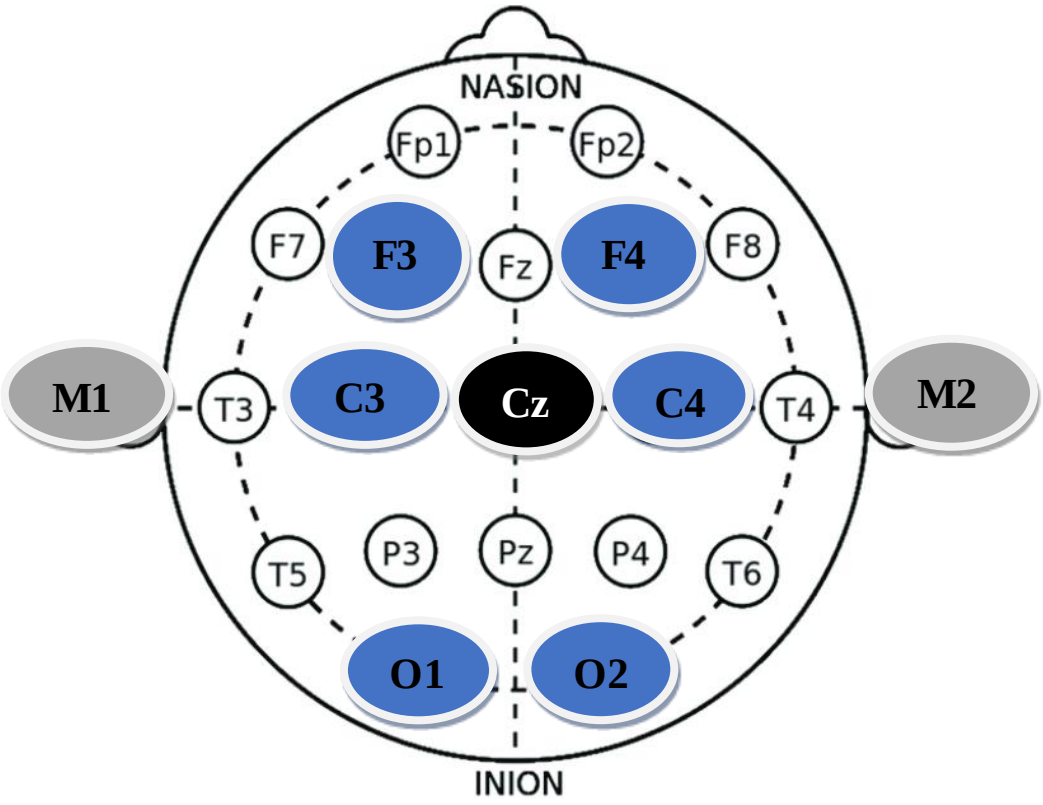

Figure 9: EEG electrode positions: Blue colour indicates frontal, central and occipital electrodes, grey colour shows reference, and black colour shows ground.

Table 2: Location of head electrodes for EEG [59]

Naison is the point at the top of nose and inion is a bump present at the base of skull that can be felt externally on the head.

Name of electrode	Location
Cz	Point of intersection at: 50% of the total distance (a) from naison to inion, 50% of the total distance (b) from left ear to the right ear
Fz	20% total distance (a) towards nose from Cz
Fpz	20% total distance (a) towards nose from Fz
Pz	20% total distance (a) towards back from Cz
Oz	20% total distance (a) towards back from Pz
C3	20% total distance (b) towards the left ear from Cz
C4	20% total distance (b) towards the right ear from Cz
T7	20% total distance (b) towards left ear from C3
T8	20% total distance (b) towards right ear from C3
Oz	50% of total circumference of the head intersecting Fpz, T7 and T8
O1	10% half-circumference towards the left ear from Oz
O2	10% half-circumference towards the right ear from Oz
Fp1	10% half-circumference towards the left ear from Fpz
Fp2	10% half-circumference towards the right ear from Fpz

F3	50% of distance from Fp1 to 50% of distance between Fp1 and 01 intersecting at C3
F4	50% of distance from Fp2 to 50% of distance between Fp2 and 02 intersecting at C4
M1	The bone behind the left ear
M2	The bone behind the right ear

3.3.1.2 Electrodes and sensors on the face and body

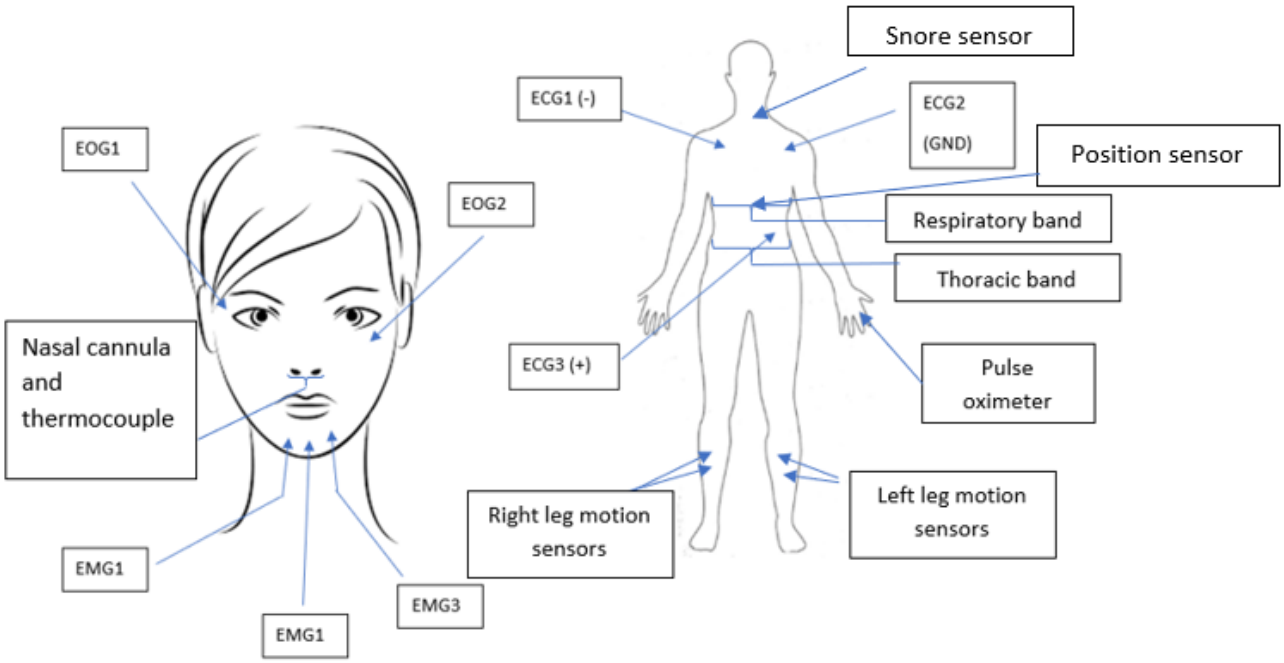

Figure 10: Electrodes and sensors on body and face [76]

Figure 2 shows the placement of electrodes and sensors on the face and body. Left and right electro-occulograms (EOG) were used for measuring eye movements; left, right and central sub-mentalis electromyograms (EMG) for chin movement, required in sleep staging; a modified lead

II electrocardiogram (ECG) to monitor heart rate and rhythm. Nasal cannula and thermocouple were used to measure nasal airflow parameters, a pulse oximeter to measure peripheral haemoglobin oxygenation, pulse rate and blood flow changes, and a snore sensor to monitor snoring. Respiratory effort was measured with bands around thorax and chest along with a position sensor to detect sleep positions (supine, prone, left and right) throughout study. Right and left leg EMG were recorded to sense leg movements.

3.3.2 NIRS data acquisition

NIRS data was acquired using the Portalite by Artinis Medical Systems (Netherlands), at a sampling rate of 10Hz. This frequency was selected for NIRS data acquisition because hemodynamic responses of our concern are well below 5 Hz [85] and using 50 Hz would mean merely a lot of memory consumption and processing time. The Portalite consists of 3 transmitters and 1 receiver with each transmitter emitting lights of wavelengths 760nm and 850 nm. Thus, there are 6 different NIRS channels, 3 corresponding to oxy-haemoglobin (HBO) and remaining 3 to de-oxyhemoglobin signal (HHB). The Portalite probe was placed on the right prefrontal region and then covered by a black headband to prevent light interference. For synchronisation with PSG, the C3 electrode and the Portalite probe were simultaneously tapped and an event marker was placed on the recording systems by the operator .

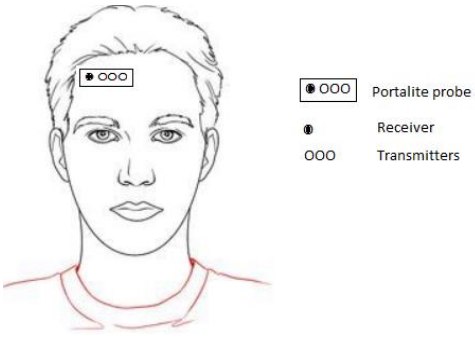

Figure 11: Portalite probe position

3.4 Data pre-processing

3.4.1 Sleep data

The PSG data was used for sleep scoring independently by trained personnel based on the guideline by AASM [71]. Whole night sleep was scored into 5 different stages: Stage Wake (W), NREM1, NREM2, NREM3 and REM stage in 30 second epochs.

3.3.2 NIRS data

3.4.2.1 Preparing NIRS data

The raw NIRS data consisted of oxy-haemoglobin and de-oxyhemoglobin signals together with total haemoglobin, differential haemoglobin, and tissue saturation factors. Firstly, only the oxyhaemoglobin (HBO) and de-oxyhemoglobin (HHB) signals were extracted from the raw NIRS data (figure 12).

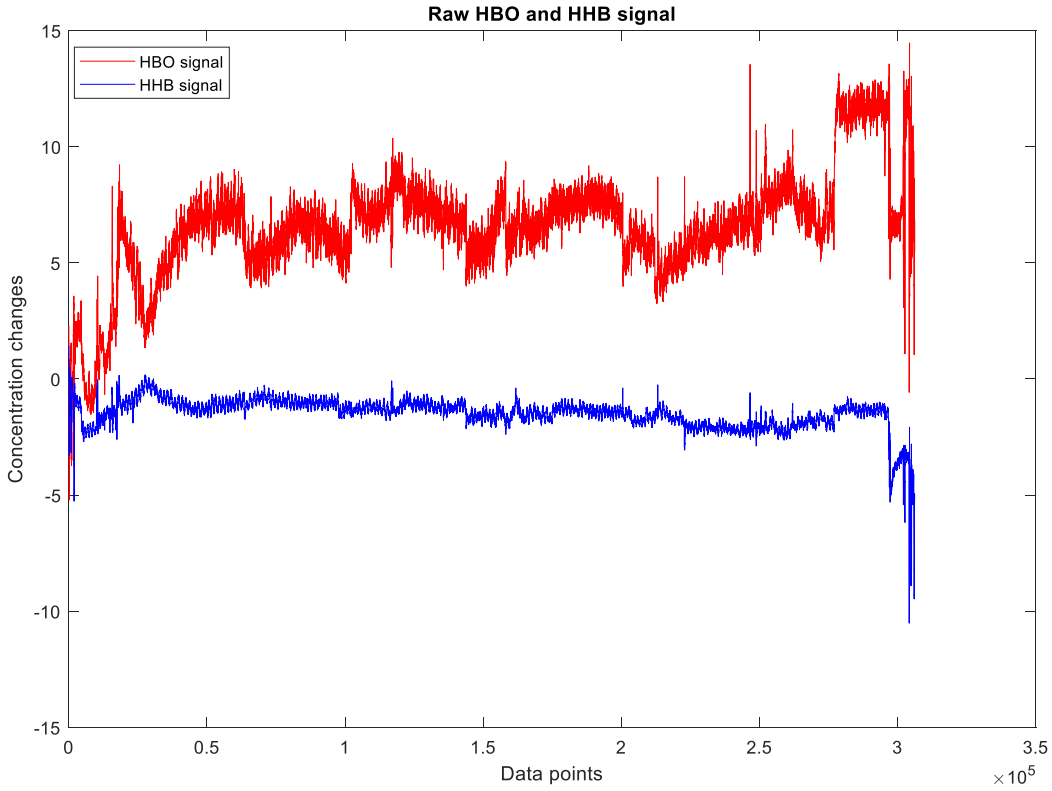

Figure 12: Raw oxyhemoglobin (HBO) and de-oxyhemoglobin (HHB) signal

3.4.2.2 Cleaning data

The NIRS raw data was subjected to a series of data cleaning tools

3.4.2.2.1 Exponential Moving Average (EMA) filter

EMA filter with a 2s short-term window and 10s long-term window was implemented to the raw NIRS signal. As shown in figure 13, random fluctuations from the HBO time series data, which

could be a form of instrument noise, have been smoothened by EMA filtering revealing the actual behaviour of the signal over time.

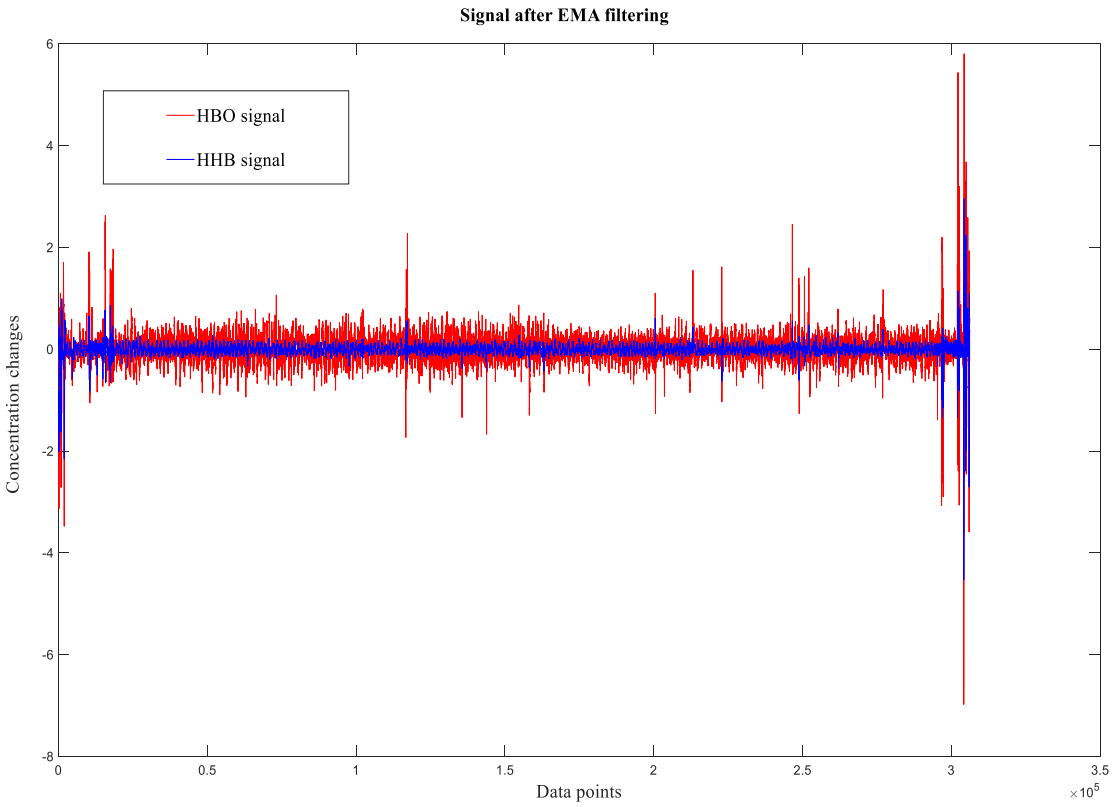

Figure 13: NIRS oxy-haemoglobin (HBO) signal after EMA filtering

3.4.2.3 Removing motion artefact using threshold method

The data was then subjected to threshold-based method of motion artefact removal using the NIRS analysis package (NAP) toolbox in MATLAB provided by Fekete et al., (2011) [65]. The threshold for spikes detection was set to 0.2 and then a Butterworth filter (order: 4, sampling rate: 10Hz, and cut-off: 0.01Hz) was applied. Similarly, thresholds of 4, 150 and 250 were set for ripple detection followed by the application of same Butterworth filter at a sampling rate of 0.1 Hz. The HBO

signal as shown in figure 14 is much smoother as the suspected artefact data points resulting from motion have been restructured from the EMA filtered signal.

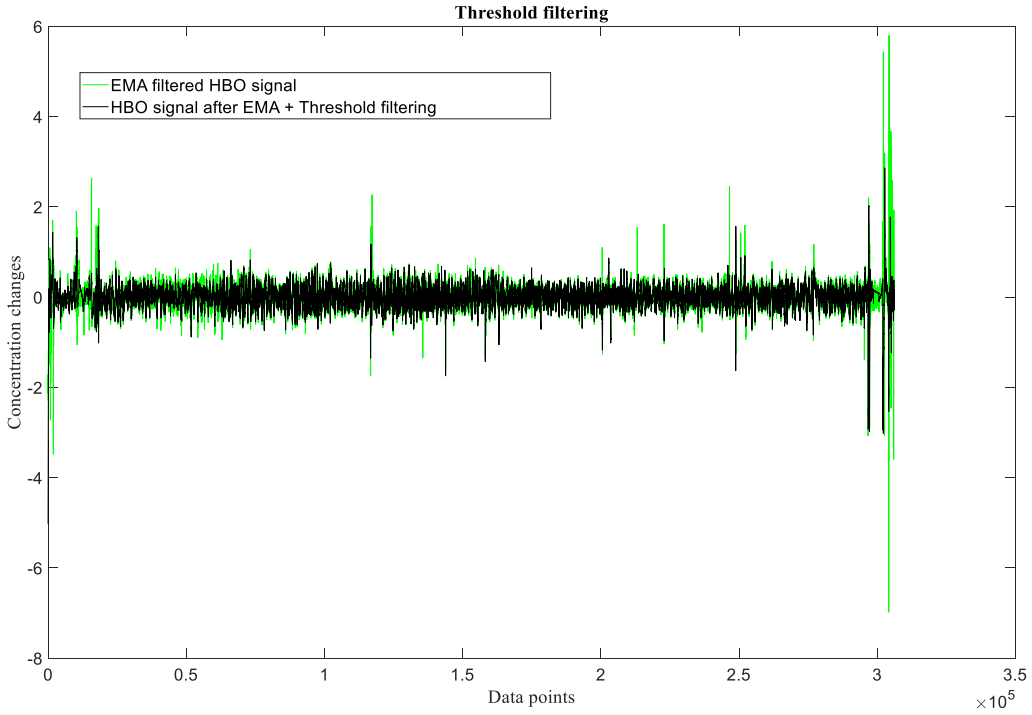

Figure 14: NIRS oxy-haemoglobin (HBO) signal after EMA + threshold filtering

3.4.2.3 Removing motion artefact based on CBI method

The signal was finally subjected to correlation-based method (figure 15) of signal improvement [67]. The result is such that HBO and HHB data are now anti-correlated (figure 17) indicating that the signal is now free from motion artefacts [67].

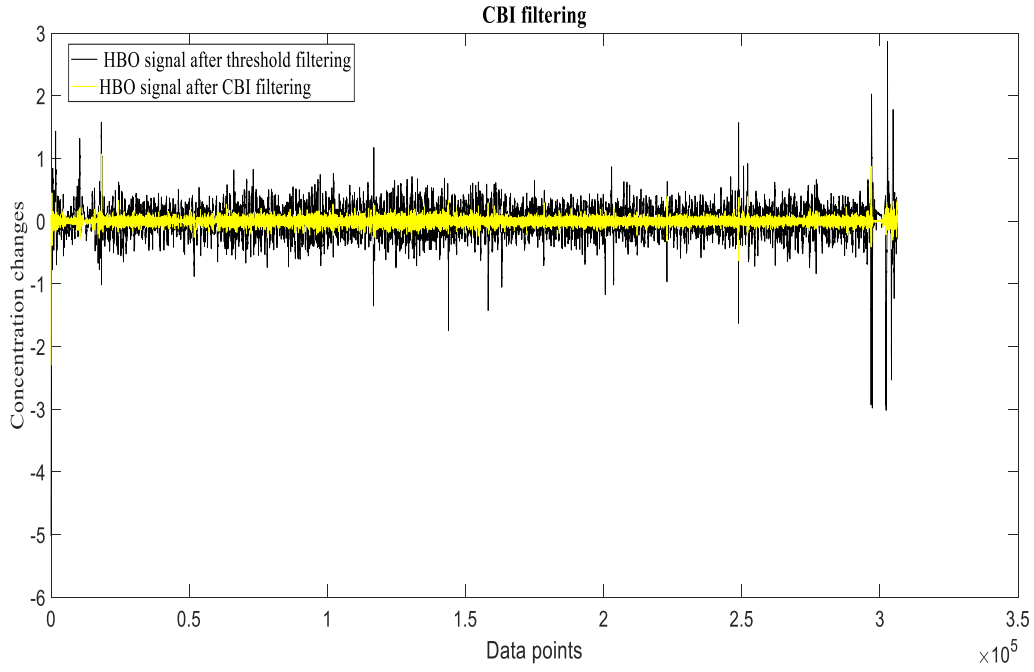

Figure 15: NIRS oxy-haemoglobin (HBO) signal after EMA + threshold + CBI filtering

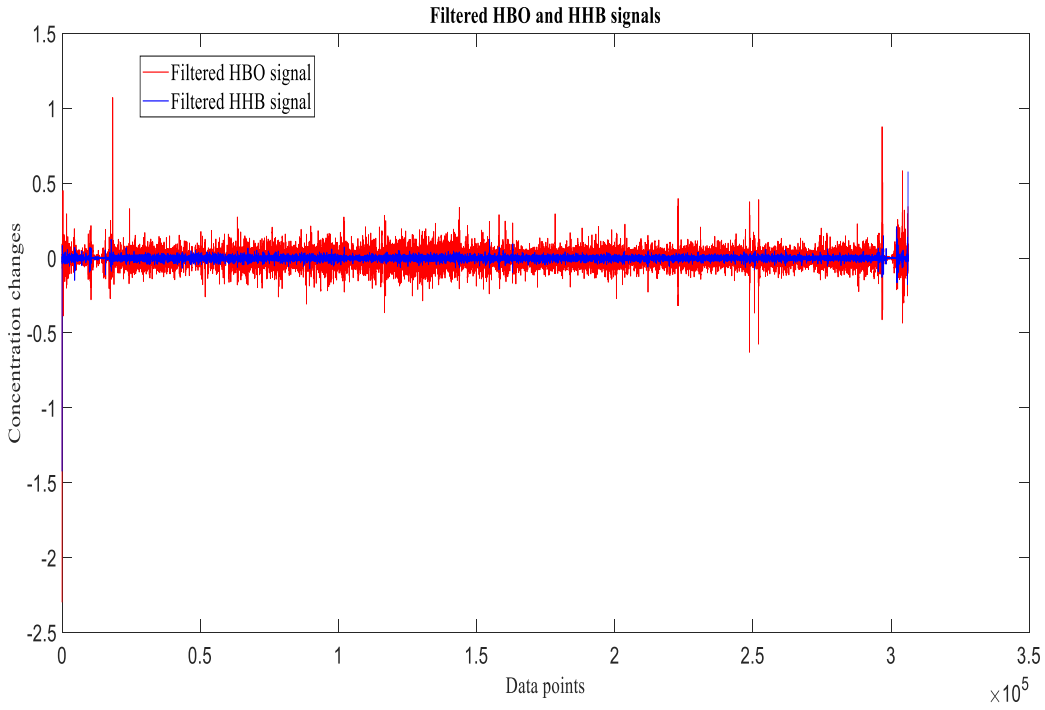

Figure 16: Clean oxyhemoglobin (HBO) and de-oxyhemoglobin (HHB) signal after filtration and signal improvement

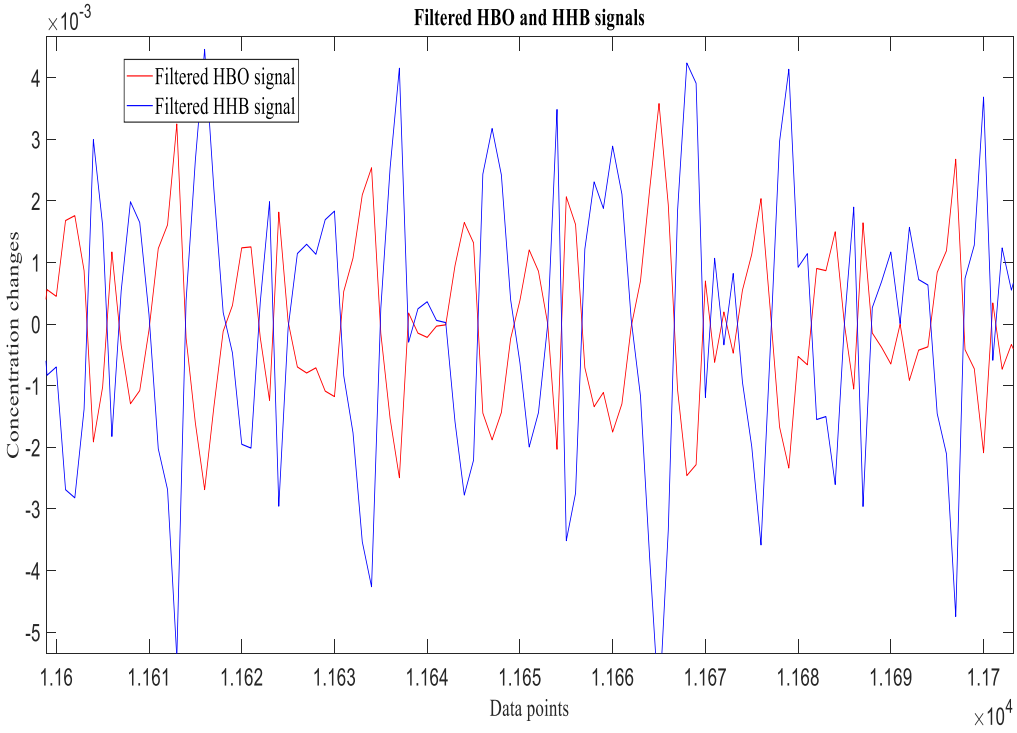

Figure 17: Anti-correlated HBO and HHB signals after CBI signal improvement

3.4.2 EEG data

EEG data was obtained as a part of the PSG and hence, the first step towards processing it was to extract only the required EEG channels from the available PSG data. Two frontal (F3-M2, F4-M1), two central (C3-M2, C4-M1), and two occipitals (O1-M2 and O2-M1) channels were labelled and cleaned using the EEGLAB toolbox and *clean_rawdata* function with default parameters in MATLAB [98]. Signal from one of the channels, O2-M1, was very noisy and was lost in the cleaning process from all subjects when using the cleaning tool. Hence, we now have 5 EEG channels and 6 NIRS channels, giving a total of 11 channels for further processing.

3.5 Data synchronisation and Segmentation

The EEG, NIRS and sleep scored data were synchronised by implementing respective time delays based on the event marker on the acquisition systems following simultaneous tapping of the C3

electrode and Portalite probe. NIRS signal was up-sampled from 10 Hz to 100Hz and EEG data was down-sampled to 100Hz using *resample* function in MATLAB. 100 Hz frequency was used for EEG signal because initially it was notch filtered at 50 Hz and having a sampling frequency twice the desired signal range ensures that the Nyquist criterion is fulfilled [118].

The EEG data was then subjected to HPF with cut-off of 0.5 Hz in order to get rid of the noises which were low frequency, baseline wanders as suggested by Palaniappan (2011) [99]. The entire dataset was then segmented by using a 10-minute window. Hereafter, an artefact mask was implemented such that any artefact containing segment is labelled 1 and a clean segment is labelled 0. The artefact mask algorithm computed the average amplitude of the signal throughout the entire length and segments with amplitude higher than the average were extracted using start and end points masking them as 1. Segments with artefacts were discarded and only clean segments were processed for connectivity measure.

3.6 Connectivity measure

Cross-correlation measure was applied to all EEG and NIRS channels in order to trace functional connectivity between the regions covered by these channels. The measure was implemented using a 100ms sliding window hence the range of lag being -100ms to +100ms. Thereafter, transfer entropy was implemented to produce an 11*11 connectivity matrix (5 EEG channels, 6 NIRS channels) for each sleep stage and subject, with different number of segments since each subject

spent variable time at various intervals in these sleep states. Thus, we have 5 (11*11* X *5) matrices for 5 sleep states, X number of segments and 5 subjects.

3.7 Experimental and Statistical analysis

3.7.1 ANOVA and post hoc t-test

According to Hilton et al., (2006), ANOVA (Analysis of variance) is a statistical method of comparing groups of data to see if these groups differ from each other to a reasonable extent [100]. A one-way ANOVA test finds the difference between two specific groups (two sleep stages in our case). The test holds the null hypothesis that means of two groups under comparison is same. A significant p –value of ANOVA test would mean that the groups under comparison aren't same and have different means, thus rejecting the null hypothesis. Higher p–values (>0.05) indicate that there is no reasonable variation among the groups, and population means might have been different by chance, whereas lower p-value (<0.05) indicates that there exists some significant differences among the group, and the difference is not merely by chance. The information provided by ANOVA test is limited to finding of existence of difference among groups but not the precise two groups which have different means. In order to find out which two groups have significant difference in their mean, post-hoc test is required.

Tukey's post-hoc test (t-test) is one of the commonly used post-hoc tests after rejecting null hypothesis in ANOVA. It is a multiple comparison test that makes a pairwise comparison between groups of interest and finds such two groups, which have their means significantly different from one another.

As a matter of fact, even when the ANOVA result is significant, one may not find any two groups of data having statistically different means from post-hoc t-tests. This is because the significance

in ANOVA test might come from combined means of two groups compared to the combined means of other two groups. Nevertheless, when we require to find out if the means of groups under analysis are different, ANOVA test and post hoc t-test seem quite useful [100].

3.7.2 Permutation test of independence

According to Good (2013), permutation test of independence is a non-parametric test that compares two groups as independent datasets and computes the difference between them [101]. The significant outcome of permutation test does not suggest a value equal to difference of medians of the two groups but rather infers that the two groups differ significantly. A p-value is obtained by resampling the data over repeated number of times. The null hypothesis is that the data are drawn from the same pool and do not have significant difference. P-value < 0.05 indicates that there exists significant difference between the group of datasets [101].

3.7.3 Experiments

In the first round, the measure was averaged over the number of segments (3rd dimension) and then over the number of subjects (4th dimension) giving five 11*11 matrices for 5 different stages of sleep. For better analysis, the adjacency matrix was extracted in smaller sizes corresponding to connectivity between EEG and oxyhemoglobin (HBO) and de-oxyhemoglobin (HHB). Furthermore, transfer entropy from EEG to HBO and HHB, and that from HBO and HHB to EEG were separately extracted to analyse connectivity between these channels individually. The output was then subjected to statistical analysis using ANOVA test. P-values below the significant level of 0.05 were considered to carry statistical significance of difference in means. The results of this experiment were not sufficient to derive any conclusion and hence we changed our path to performing a non-parametric randomisation test.

In the second round, the sleep stages for all subjects were concatenated together and a permutation test was carried out (significant for p-value< 0.05). For datasets with significant p-value, the connectivity was plotted on the head using 5 EEG channels and 3 locations corresponding to approximate position of NIRS sensors on the NIRS probe. The arrow on the plot shows the direction of connectivity.

It was found that randomisation test (permutation) is more effective in catching up the details in data sets than statistical ANOVA test and that could be because of the small dataset obtained from 5 subjects.

Chapter 4 : Connectivity between EEG and NIRS channels

4.1 Connectivity between EEG and oxyhemoglobin (HBO) channels

For average connectivity over number of subjects, adjacency matrices were extracted individually for connectivity from EEG to NIRS channels and vice versa. It was clearly evident that causal influence from NIRS channels to EEG channels was stronger than that from EEG channels to NIRS channels, as derived from both HBO and HHB. However, upon ANOVA analysis, no significant difference between the connectivity in the 5 sleep stages was found between any of the EEG and NIRS channels.

4.1.1 Measuring transfer entropy from HBO channels to EEG channels

The connectivity matrices extracted for transfer entropy from HBO to EEG channels showed increasing values from wake stage to NREM1 stage but decreasing in NREM2 stage (figure 18). Comparing NREM3 and REM stage, the connectivity is higher in the former stage. In short, there seems to exist rise-fall trend in connectivity throughout these sleep stages.

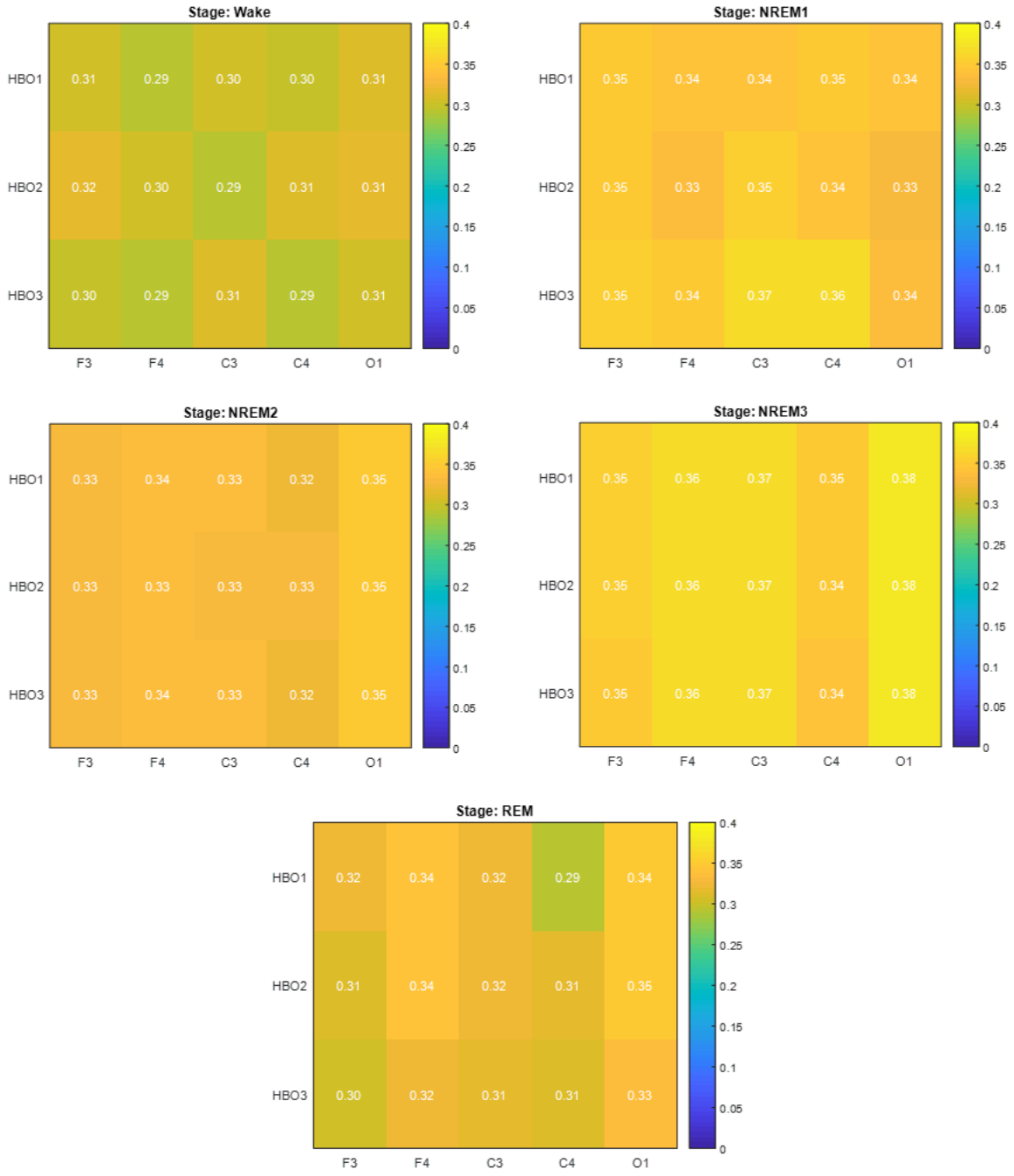

Figure 18: Connectivity matrices for transfer entropy from HBO to EEG channels

ANOVA results were insignificant with p-value of 0.7575 (figure 19). Hence, we cannot draw out any conclusion regarding the connectivity changes at this point.

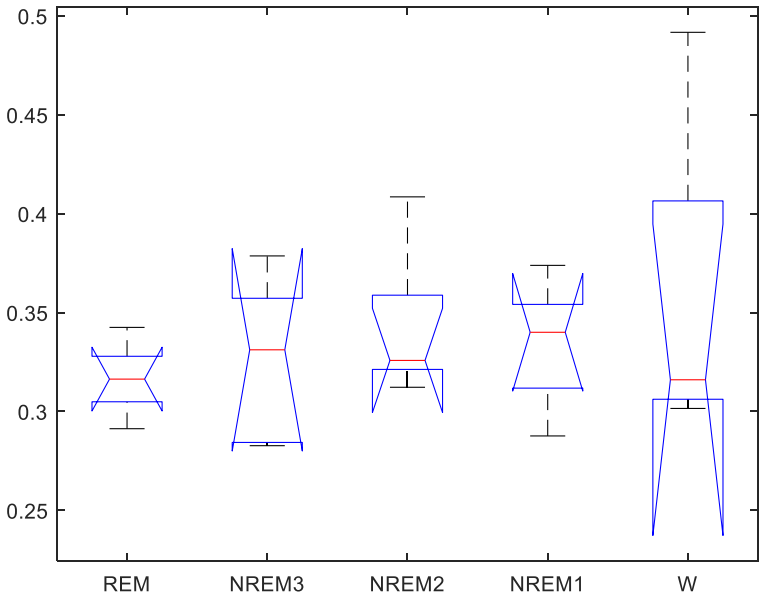

Source	SS	df	MS	F	Prob>F
Groups	0.00425	4	0.00106	0.47	0.7575
Error	0.04302	19	0.00226		
Total	0.04727	23			

Figure 19: ANOVA results for transfer entropy measure from HBO to EEG channels

4.1.2 Measuring transfer entropy from EEG channels to HBO channels

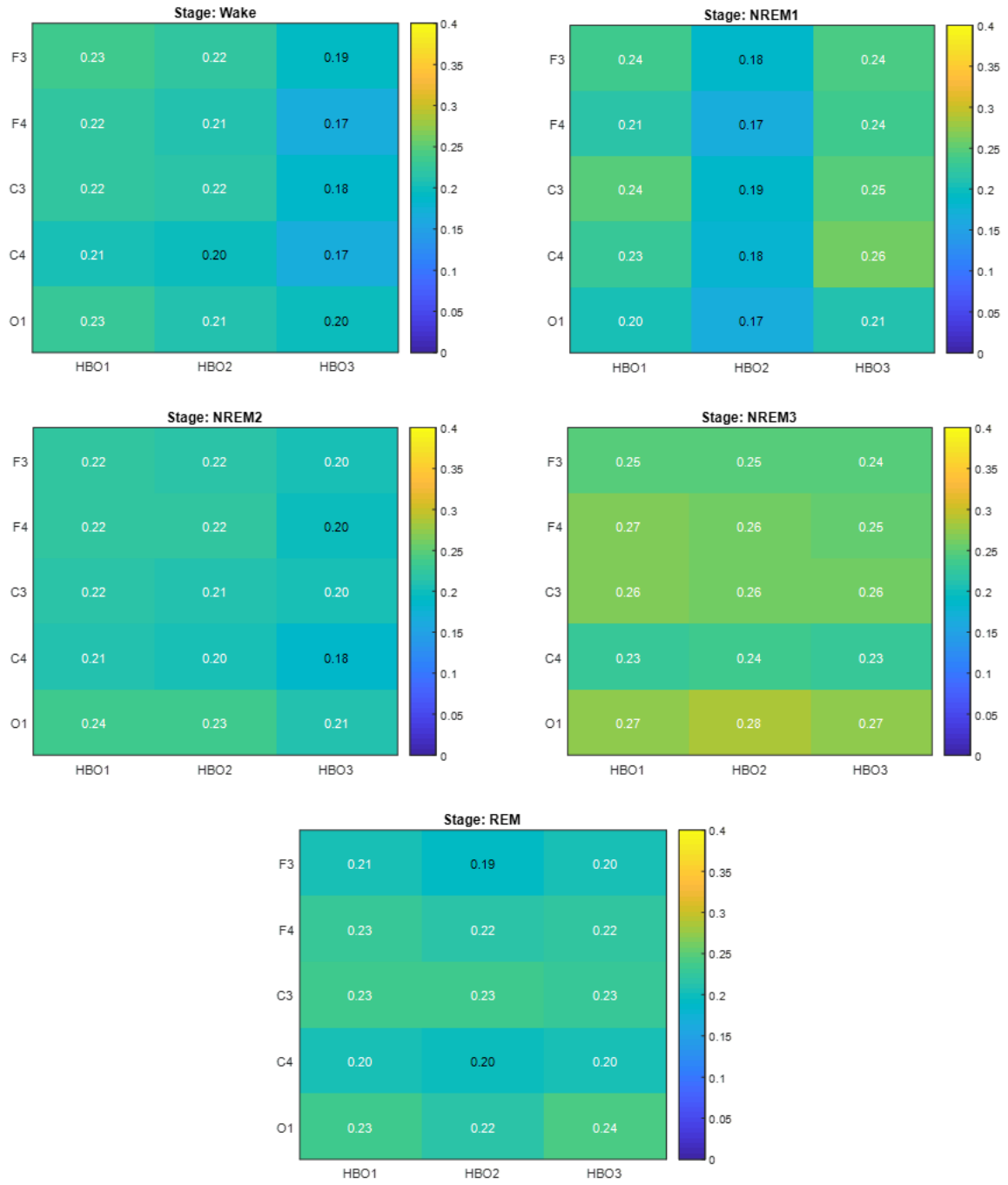

Figure 20: Connectivity matrices for Transfer entropy measure from EEG to HBO channels

It can be seen that the connectivity values are lower when directed from EEG to HBO channels (figure 20) than vice versa (figure 18). This suggests that the information flow is strong in the

direction of HBO to EEG channels. Besides this, no conclusion can be derived in relation to connectivity across different sleep states as the statistical test was insignificant as shown in (figure 21).

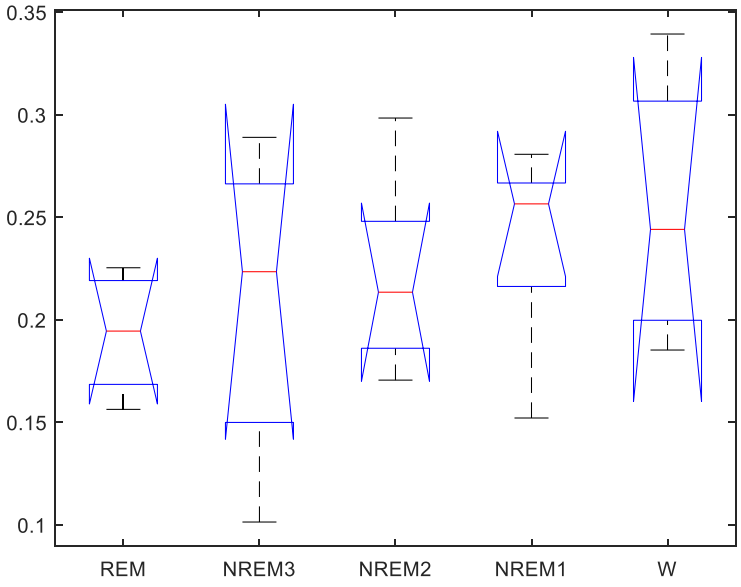

Source	SS	df	MS	F	Prob>F
Groups	0.01031	4	0.00258	0.82	0.5269
Error	0.05956	19	0.00313		
Total	0.06987	23			

Figure 21: ANOVA results for transfer entropy measure from EEG to HBO channels

4.1.3 Connectivity during wake stage compared to NREM1, NREM2, NREM3 and REM sleep

Although the statistical ANOVA test was insignificant, when the connectivity during all sleep stages were concatenated for all subjects and a permutation test was carried out so as to measure the difference in connectivity between every other sleep stage, significant results were obtained as seen on the head plot. The plots indicate overall network of casual influence between EEG and NIRS channels (HBO and HHB).

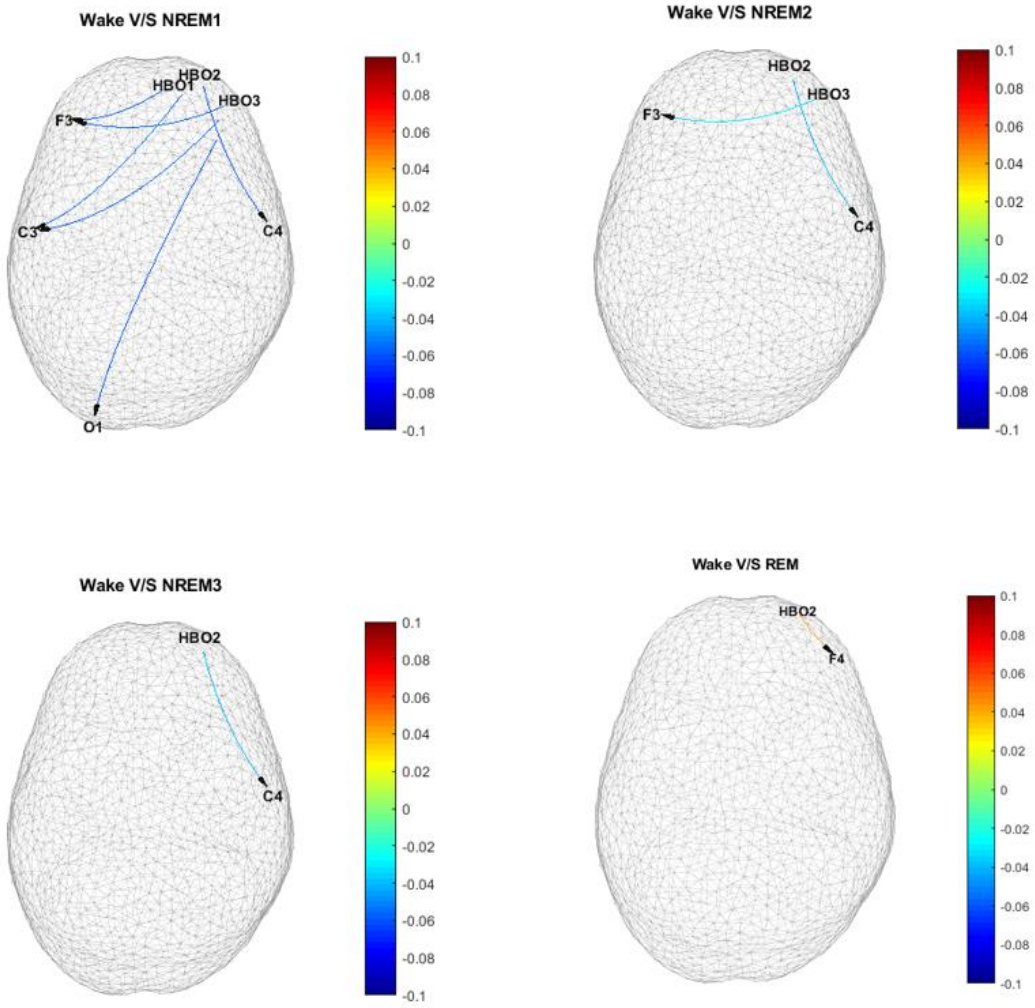

Figure 22: Connectivity during wake stage compared to NREM1, NREM2, NREM3 and REM sleep

4.1.3.1 Significant findings

Overall, whole brain connectivity during wake stage is less than that in NREM1 stage and connectivity between frontal and central region in wake is less than that in NREM2 and NREM3 stage.

4.1.3.2 Discussion

The comparison between wake and NREM1 state clearly shows that the whole brain connectivity is lower in wake stage as compared to that in NREM1 stage. As suggested by fewer number of networks, connectivity during wake is less than that in NREM2 and NREM3, but greater than in REM stage. This finding of ours when compared to literature shows that the finding is consistent with respect to NREM1, NREM2 but contradicts in case of NREM3 as found by Tagliazucchi et al., (2014) that connectivity during wake is less than that in NREM1 and NREM2 but greater than that in NREM3 [102]. The difference could be better concluded with a greater number of networks revealing the difference.

4.1.4 Connectivity during NREM1 stage compared to NREM2, NREM3 and REM sleep

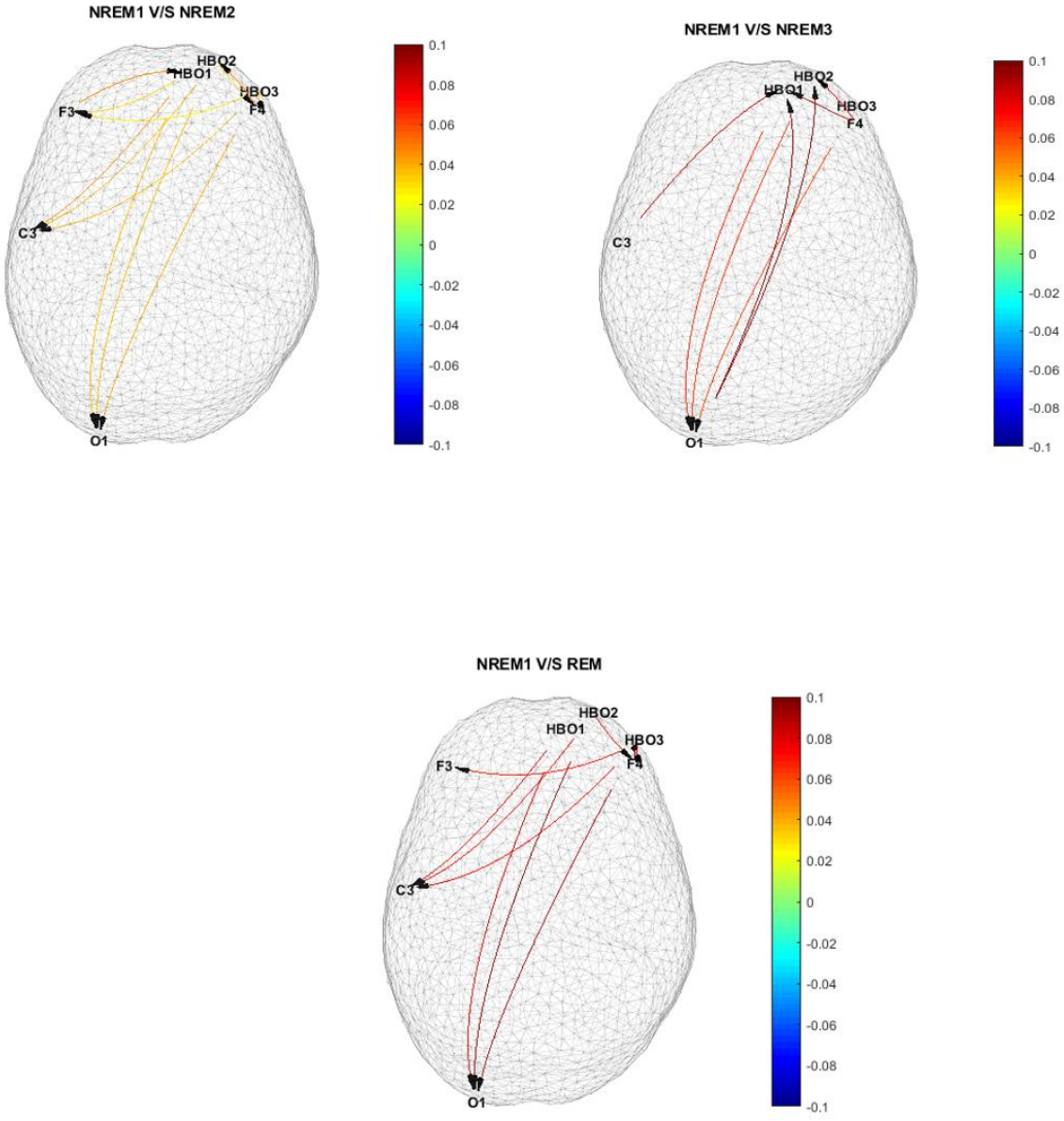

Figure 23: Connectivity during NREM1 stage compared to NREM2, NREM3 and REM

4.1.4.1 Significant findings

1. Effective connectivity from HBO channels to O1 is greater in NREM1 stage than NREM2, NREM3 and REM stage. Further, the difference between connectivity in NREM1 and the other stage is increasing from NREM2 to REM as:

   (NREM1-REM) > (NREM1-NREM3) > (NREM1-NREM2)
2. Effective connectivity from HBO channels to C3 is highest in NREM1 satge such that:

   (NREM1-NREM2) > (NREM1-REM)
3. There is the existence of a feedback loop from
   i. F3 to HBO1 and F4 to HBO2 which is stronger in NREM1 stage than NREM2.
   ii. Also from O1 to HBO1 and HBO2 which is stronger in NREM1 than NREM3.
   iii. Aalso from F4 to HBO3 which is stronger in NREM1 than REM.
4. As comapred to NREM3, effective connectivtiy from O1, C3 and F4 channels to HBO channels is greter in NREM1 stage. The difference in this directionality is barely present when NREM1 is compared to other sleep stages.

4.1.4.2 Discussion

4.1.4.2.1 Feedback loop in NREM sleep

The persistence of feedback loops in NREM sleep connectivity network is interesting. It can be related to the cortico-thalamic-cortical loop involved in regulating sleep spindles, K-complexes and slow wave activity during NREM sleep [103, 104, 105].

According to Krone et al., (2017), a pathway involved in regulating sleep-wake cycle is the bottom-up pathway that originates in the brainstem and propagates along thalamo-cortical region [106]. During NREM sleep, the anterior cortical areas are least activated as compared to the wake stage giving rise to slow wave oscillations between cortex and thalamus [107]. These slow wave

oscillations are travelling waves that propagate from frontal to posterior brain regions [103]. On the same side, the occasional bursts of sleep spindles and K-complexes in NREM sleep are regulated by a loop existing over thalamo-cortical route: the thalamo-cortico-thalamic loop [105]. Additionally, Steriade, M., (2003) suggested that instances of sleep spindles correspond to the maximum blockage of afferent signals to the cortex preventing a person from being aware of the environment [104] indicating why a person loses consciousness on onset of NREM sleep.

Migliorelli et al., (2019) suggested that a measure of brain connectivity is related to the loop of slow wave regulation along with periodic appearances of sleep spindles and K-complexes [108]. As such, we could hypothesise that the connectivity directed from frontal to central and occipital regions could correspond to the propagation of slow waves in NREM sleep and the appearance of feedback loops in the connectivity plot corresponds to cortico-thalamic-cortical loop involved in regulation of sleep spindles and K-complexes. Our findings could be strengthened and validated with measurements done with stereo EEG providing direct thalamic measurements rather than from scalp electrodes.

4.1.4.2.2 Brain connectivity decreases in NREM2 stage

It is evident that the brain connectivity in NREM2 stage decreases as compared to NREM1 stage and can be claimed to be statically significant since the head plot comes from only significant p-values of permutation test. It is also observed that effective connectivity in brain from right prefrontal region (considering all NIRS channels) to left occipital region (O1) is highest during NREM1, followed by NREM2, NREM3 and least during REM stage of sleep. Furthermore, the connectivity between these channels seems to fairly decrease along NREM2, NREM3 and REM stage based on simple algebra of increasing difference in the connectivity during these states as compared to NREM1 stage, although further statistical validation would be required to give a

strong conclusion. Jurysta et al., (2012) demonstrated using only EEG signals that information flow to posterior brain regions follow a decreasing trend as sleep progresses from NREM1 to NREM3 which is similar to our finding of decreasing entropy transfer along these states [109]. The fact that functional connectivity decreases in NREM2 stage has been depicted by Migliorelli et al., (2019), though the findings could not compare in relation to effective connectivity [108].

4.1.5 Connectivity during NREM2 stage compared to NREM3 and REM

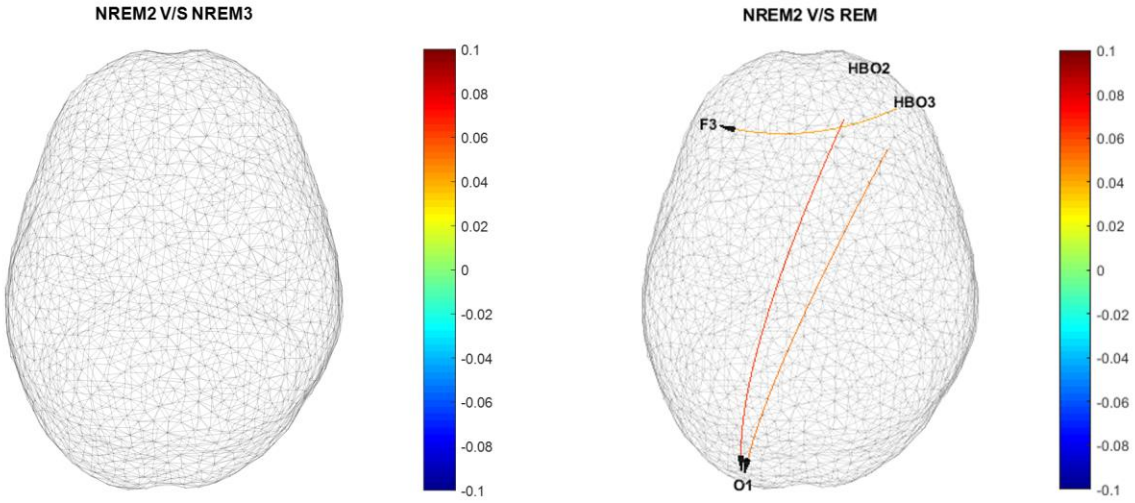

Figure 24: Connectivity during NREM2 stage compared to NREM3 and REM

4.1.5.1 Significant findings

1. No significant difference between NREM2 and NREM3.
2. As compared to REM, connectivity from HBO channels to F3 and O1 is higher in NREM2.

4.1.5.2 Discussion

As obtained from comparing NREM1 stage with NREM2 and NREM3, connectivity during NREM1> NREM2, and NREM1> NREM3. But when we compare NREM2 and NREM3 directly,

no statistically significant difference was found between the connectivity during these two states. Hence, the relation between connectivity during NREM2 and NREM3 cannot be stated accurately, although it can be expected for NREM2 stage to have higher connectivity than NREM3 based on simple algebra and literature [8].

Comparing NREM2 with REM stage, we may notice that the number of networks has been reduced compared to previous plots of NREM1 stage. However, frontal to occipital connectivity is greater in NREM2 stage than in REM stage.

4.1.6 Connectivity during NREM3 compared to REM

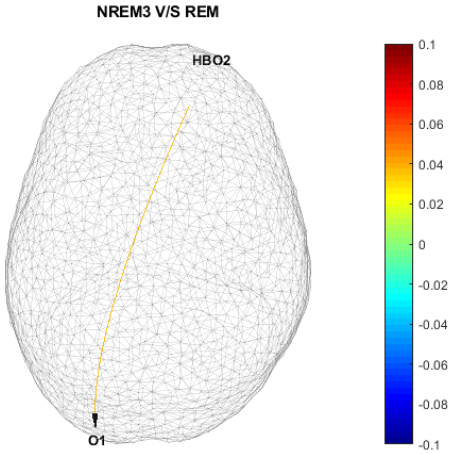

Figure 25: Connectivity during NREM3 compared to REM

It can be seen that the number of networks with statistically significant difference in connectivity is only one. However, it reveals that the connectivity from HBO2 channel to O1 in NREM3 stage is greater than that in REM.

4.1.7 Conclusion

Whole brain connectivity is highest during NREM 1 sleep stage as compared to wake or any other sleep stages. The difference between connectivity during NREM2 and NREM3 stages cannot be concluded in terms of statistical significance, though it can be anticipated that NREM2 shows higher connectivity than NREM3. Finally, there are lesser number of networks to compare connectivity during REM sleep with wake to NREM stages. One channel revelation indicates that frontal to occipital connectivity in NREM3 stage is greater than in REM sleep. As such, our findings suggest that connectivity decreases as sleep progresses form NREM to REM sleep.

4.2 Connectivity between EEG and de-oxyhemoglobin (HHB) channels

4.2.1 Measuring transfer entropy from HHB channels to EEG channels

The connectivity results derived from HHB to EEG channels were in agreement with that obtained from HBO to EEG indicating rising and falling trends in connectivity throughout sleep (figure 26).

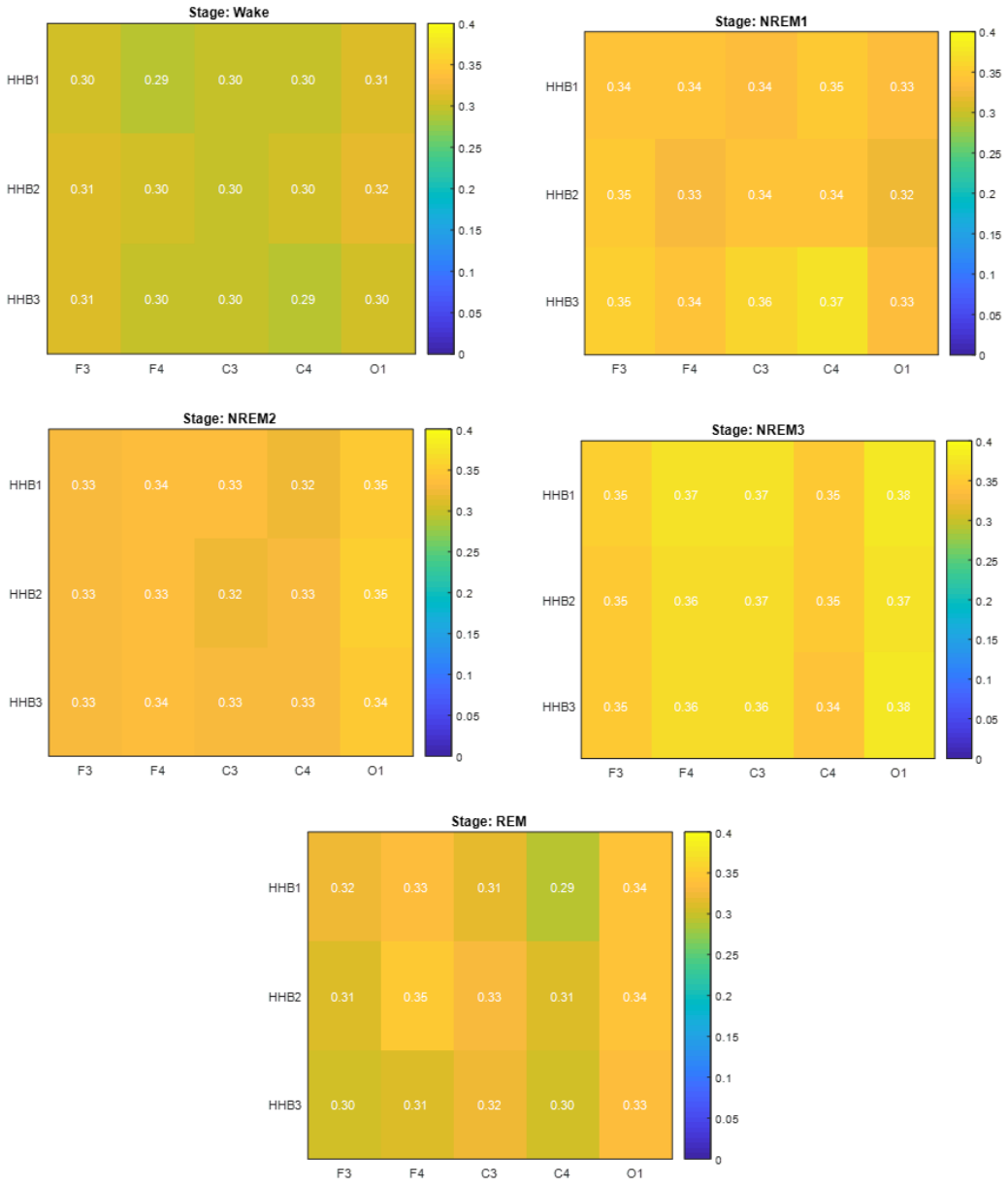

Figure 26: Connectivity matrices for transfer entropy from HHB to EEG channels during different sleep stages.

The statistical ANOVA test is still insignificant with a p-value of 0.7544 so that no dervations can be made on connectivity changes along sleep states.

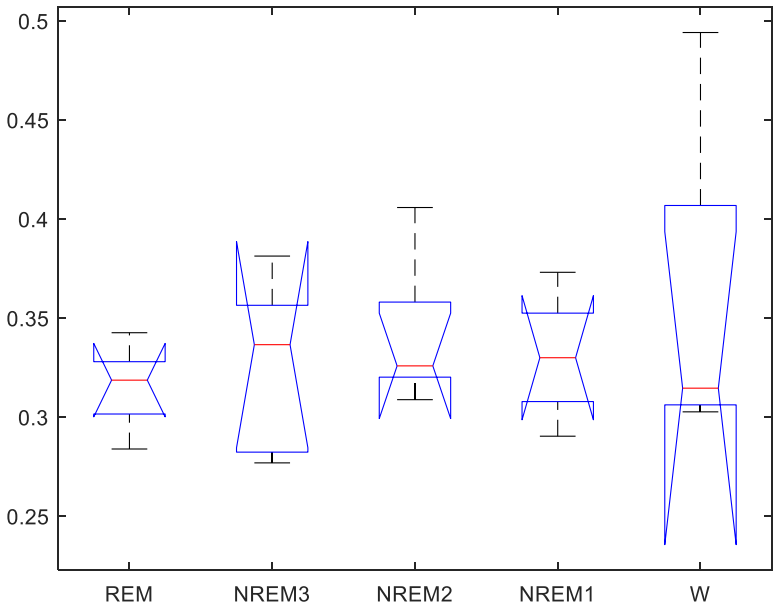

Source	SS	df	MS	F	Prob>F
Groups	0.00447	4	0.00112	0.47	0.7544
Error	0.04478	19	0.00236		
Total	0.04924	23			

Figure 27: ANOVA results for transfer entropy from HHB to EEG channels during different sleep stages

4.2.2 Measuring transfer entropy from EEG channels to HHB channels

HHB channel derivations (figure 28) for transfer entropy measure averaged over number of subjects resembles the findings from HBO channel (figure, with similar pattern (figure 20).

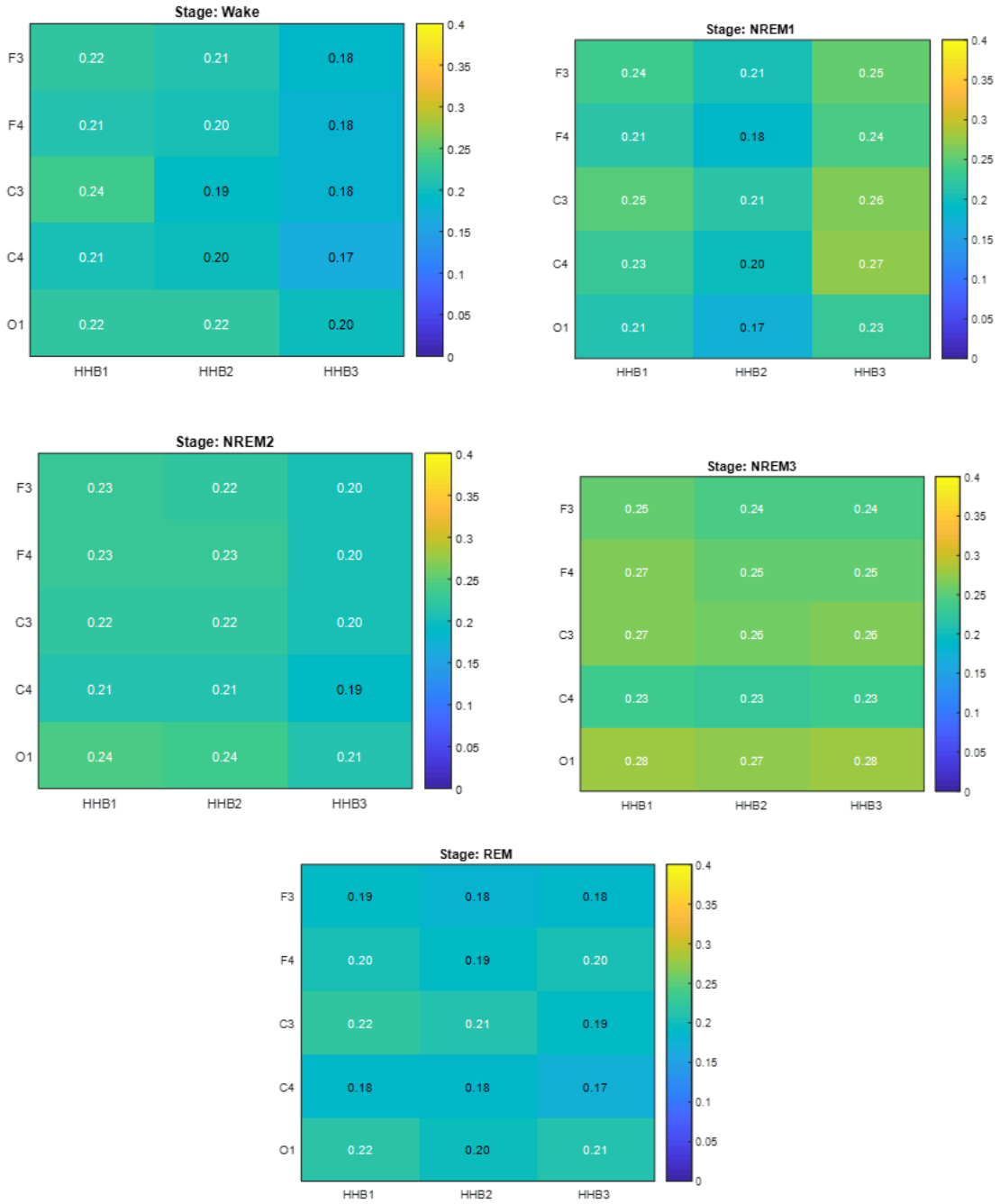

Figure 28: Connectivity matrices for transfer entropy form EEG to HHB channels

The general pattern of connectivity difference can be seen in figure (29) although the facts are not statistically significant. In conclusion, ANOVA analysis for subject averaged connectivity between EEG and all NIRS channel merely indicates that connectivity is highest in NREM1 stage as seen in general pattern. But the actual differences need more rigorous tool to find out actual significance.

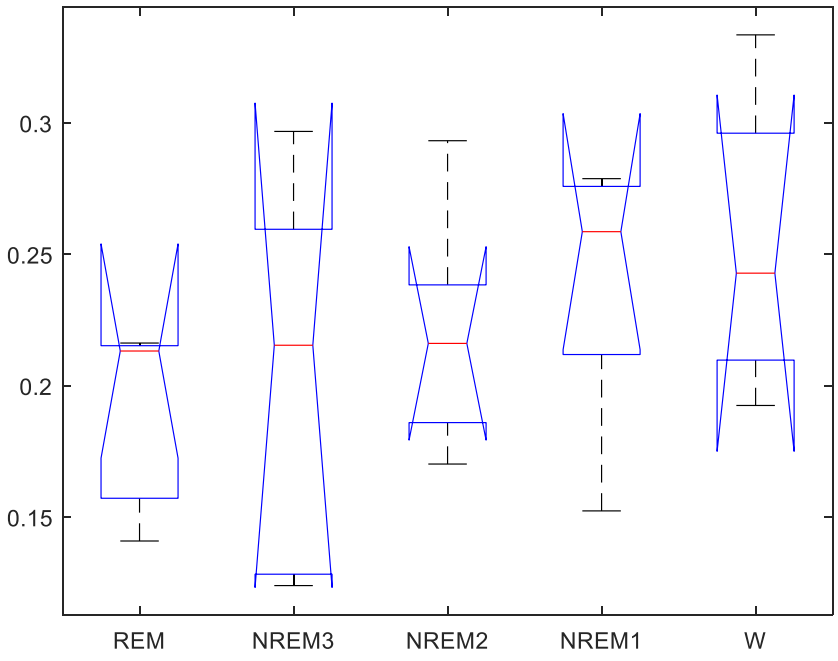

Source	SS	df	MS	F	Prob>F
Groups	0.01234	4	0.00308	1.01	0.4256
Error	0.05787	19	0.00305		
Total	0.0702	23			

Figure 29: ANOVA results for transfer entropy from EEG to HHB channels

4.2.3 Connectivity during wake stage compared to NREM1, NREM2, NREM3 and REM sleep

The findings derived from permutation test of transfer entropy measure HHB channels are similar to that derived from HBO channels except a few forms of information that only HHB channels derived.

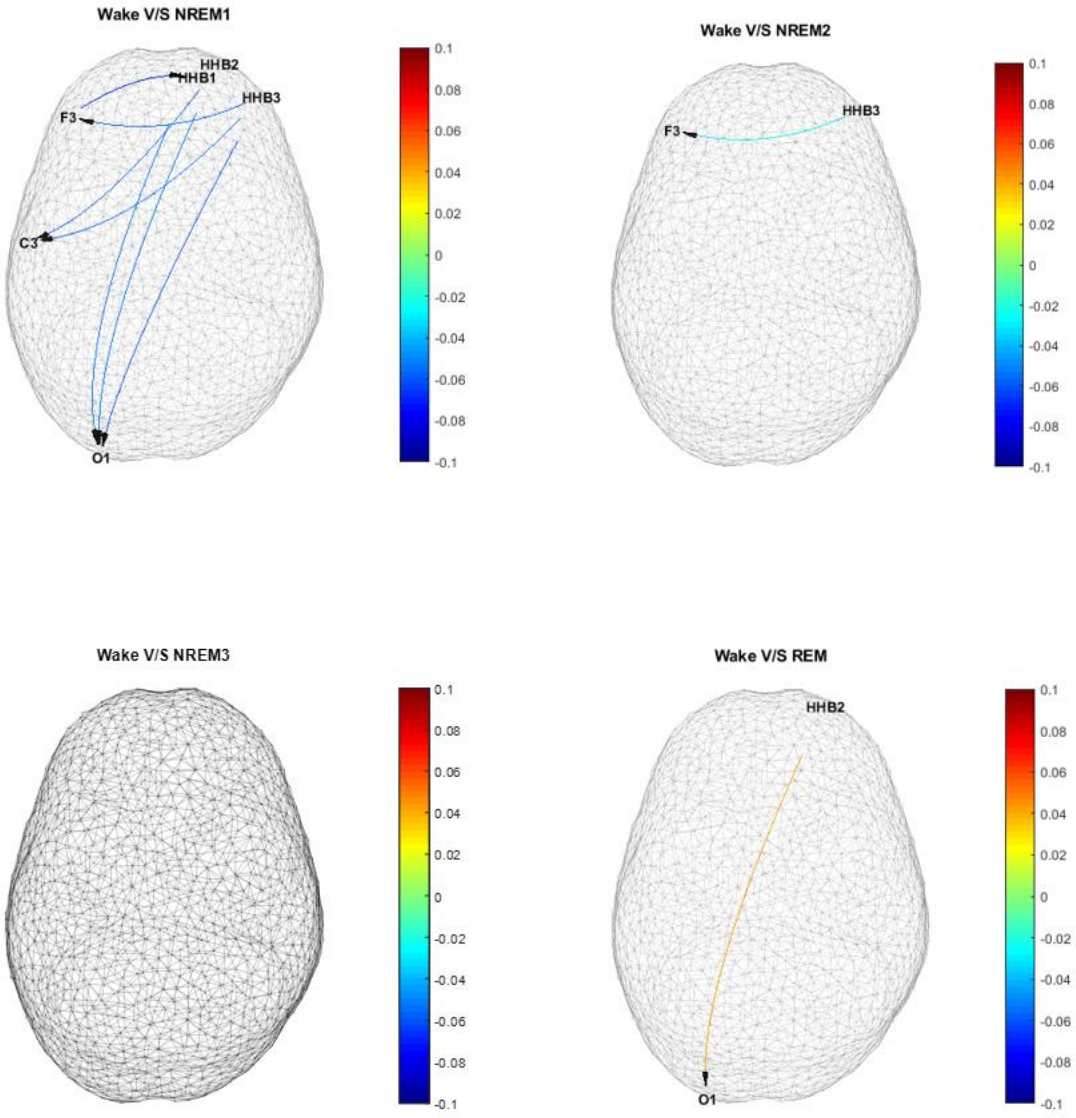

Figure 30: Connectivity derived from HHB during wake compared to NREM1, NREM2, NREM3 and REM

Connectivity during wake is less than that in NREM2, while no statistically significant difference can be seen from that of NREM3. Interestingly, the greater effective connectivity during wake as compared to REM from frontal HHB channel to occipital region has been revealed here.

4.2.4 Connectivity during NREM1 stage compared to NREM2, NREM3 and REM sleep

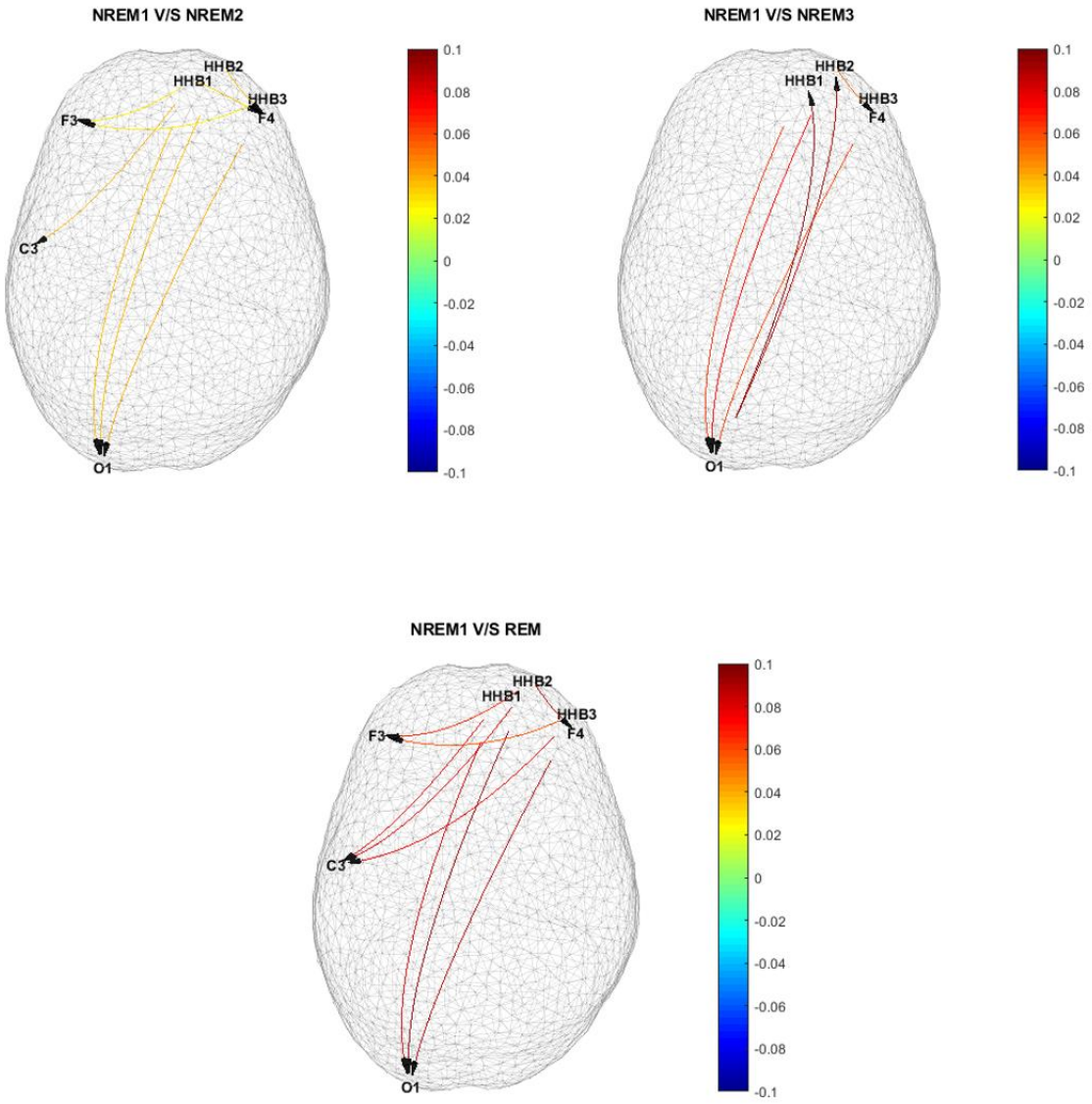

Figure 31: Connectivity derived from HHB during NREM1 stage compared to NREM2, NREM3 and REM

The findings are similar to that from HBO channels with a feedback loop prominent in NREM1 stage compared to NREM3.

4.2.5 Connectivity during NREM2 stage compared to NREM3 and REM

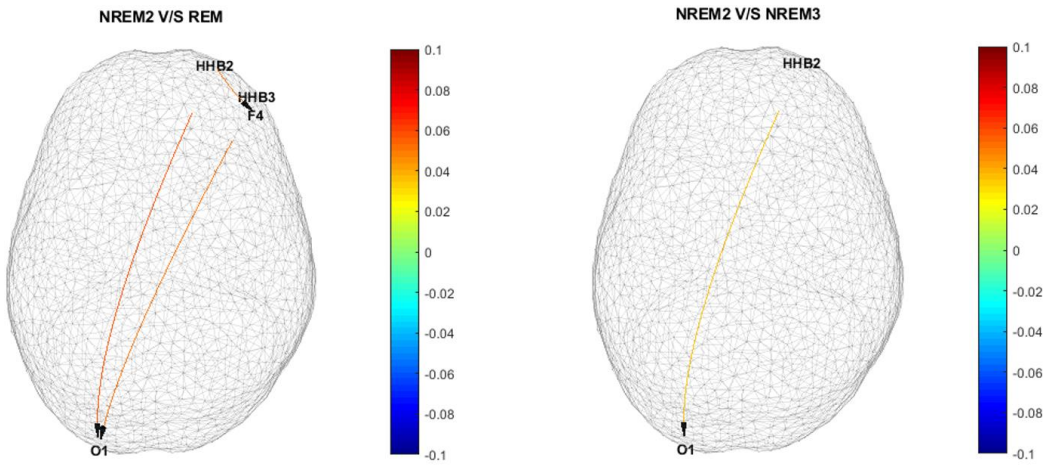

Figure 32: Connectivity derived from HHB during NREM2 stage compared to NREM3 and REM

NREM2 stage shows greater connectivty than REM stage which is consistent with the finding from HBO channels. Comparing NREM2 and NREM3, it can also be seen that frontal to occipital conncetivity is greater in NREM2 stage as compared to NREM3. Finally, we may conclude that our findings suggest connectivity decreases from NREM1 sleep to REM sleep, specifically from right pre-frontal region to left occipital region.

4.2.6 Connectivity during NREM3 compared to REM

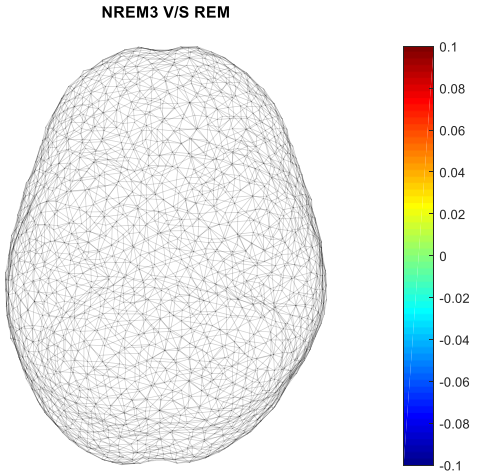

Figure 33: Connectivity derived from HHB during NREM3 stage compared to and REM

No significant difference can be found in the connectivity during NREM3 and REM stage from HHB signal derivation (figure 33) while HBO derivations (figure 25) suggested that NREM3 has higher connectivity than REM from one connection along HBO to O1.

4.3 Channel specific causal influence

A summary of important results from the obtained head plot is tabulated below:

Table 3: Directed causality from NIRS channels to EEG channels

Difference in effective connectivity (EC) between sleep stages	Symbolic representation	Referring channels and direction	
		Derived from HBO	Derived from HHB

EC in wake stage is less than that in NREM1, NREM2, NREM3 stage and greater than that in REM stage	W < NREM1	HBO1 to F3 HBO2 to C3 and C4 HBO3 to F3, C3 and O1	HHB1 to C3 and O1 HHB2 to O1 HHB3 to F3, C3 and O1
	W < NREM2	HBO2 to C4 HBO3 to F3	HHB3 to F3
	W < NREM3	HBO2 to C4	-
	W > REM	HBO2 to F4	HHB2 to O1
EC in NREM1 stage is greater than that in NREM2, NREM3 and REM stage	NREM1> NREM 2	HBO1 to F3, C3 and O1 HBO2 to F4 , C3, O1 HBO3 to F4, F3, C3, O1	HHB1 to F3, F4, C3 and O1 HHB2 to F4 and O1 HHB3 to F3 and O1
	NREM1 > NREM 3	HBO1 to O1 HBO2 to O1 HBO3 to O1	HHB1 to O1 HHB2 to O1, F4 HHB3 to O1
	NREM 1> REM	HBO1 to C3, O1 HBO2 to C3, F4, O1 HBO3 to F3, F4C3, O1	HHB1 to F3, C3, O1 HHB2 to F4, C3, O1 HHB3 to F3, C3, O1
	NREM2 > NREM 3	-	HHB 1 to F4 and O1

EC in NREM2 stage is greater than that in NREM3 and REM stage			HHB 2 to O1 HHB 3 to O1
	NREM2 > REM	HBO2 to O1 HBO3 to F3, O1	HHB2 to F4, O1 HHB3 to O1
EC in NREM3 stage is greater than that in REM stage	NREM3 > REM	HBO2 to O1	-
EC in wake stage (W) is greater than that in REM stage	W > REM	HBO2 to F4	HHB2 to O1

While most of the channels were accompanied by predominant effective connectivity from prefrontal to central and occipital region, some channels showed significant difference in connectivity directed in the opposite direction, i.e., from central and occipital region to prefrontal region:

Table 4: Directed causality from EEG channels to NIRS channels

Difference in effective connectivity (EC) between sleep stages	**Symbolic representation**	**Referring channels and direction**	
		Derived from HBO	**Derived from HHB**

EC in wake stage (W) is less than that in NREM1 stage (N1)	W < NREM1	-	F3 to HHB1
EC in NREM1 stage (N1) is greater than that in NREM2 stage (N2)	NREM1> NREM 2	F3 to HBO1 F4 to HBO 2	-
EC in NREM1 stage (N1) is greater than that in NREM2 stage (N3)	NREM1> NREM 3	F4 to HBO1 and HBO2 C3 to HBO1 O1 to HBO1 and HBO2	O1 to HHB1 and HHB 3
EC in NREM1 stage (N1) is greater than that in REM stage (R)	NREM 1 > REM	F4 to HBO3	-

Effective connectivity from occipital region to prefrontal region is higher in NREM1 stage of sleep than NREM3, REM and wake stage. Also, effective connectivity from central region to prefrontal is higher in NREM1 stage than NREM2 and REM stages.

4.3 Cross-correlation between EEG and NIRS channels

No cross-correlation was found between EEG channels and any of the NIRS channels. However, this does not indicate absence of relation between EEG and NIRS signals. This can be explained by the fact that the cross-correlation measure is applied using a 100ms sliding window and the

difference in speed of neuronal conductions (generally 50-60 m/s) are higher than hemodynamic changes (about 60 cm/seconds) so that the relation cannot be traced [110, 111]. As a result, we get a connectivity matrix with 0 value for each element.

4.4 Conclusion

The information derived from HHB channels are in agreement with that from HBO channels except a few differences in specific channels depicting the connectivity. However, the inferences that we could make froth ese derivations remain pretty much the same. HHB derivations also show that NREM2 stage has higher connectivity than NREM3 which couldn't be otherwise detected. The findings further strengthen that connectivity during sleep decreases as we proceed from NREM to REM sleep.

Chapter 5 : Connectivity between NIRS channels

Cross-correlation was applied as a measure of connectivity to the NIRS and EEG signals. The connectivity was averaged over number of segments where each sleep stage occurred and then over the number of subjects. The connectivity matrix for NIRS channels was extracted separately for HBO and HHB.

5.1Cross-correlation between oxyhemoglobin (HBO) channels

The cross-correlation between HBO channels was found to be increasing form wake stage through NREM1 stage to NREM2 stage and then decreasing in NREM3 stage (slow wave sleep) (figure 34).

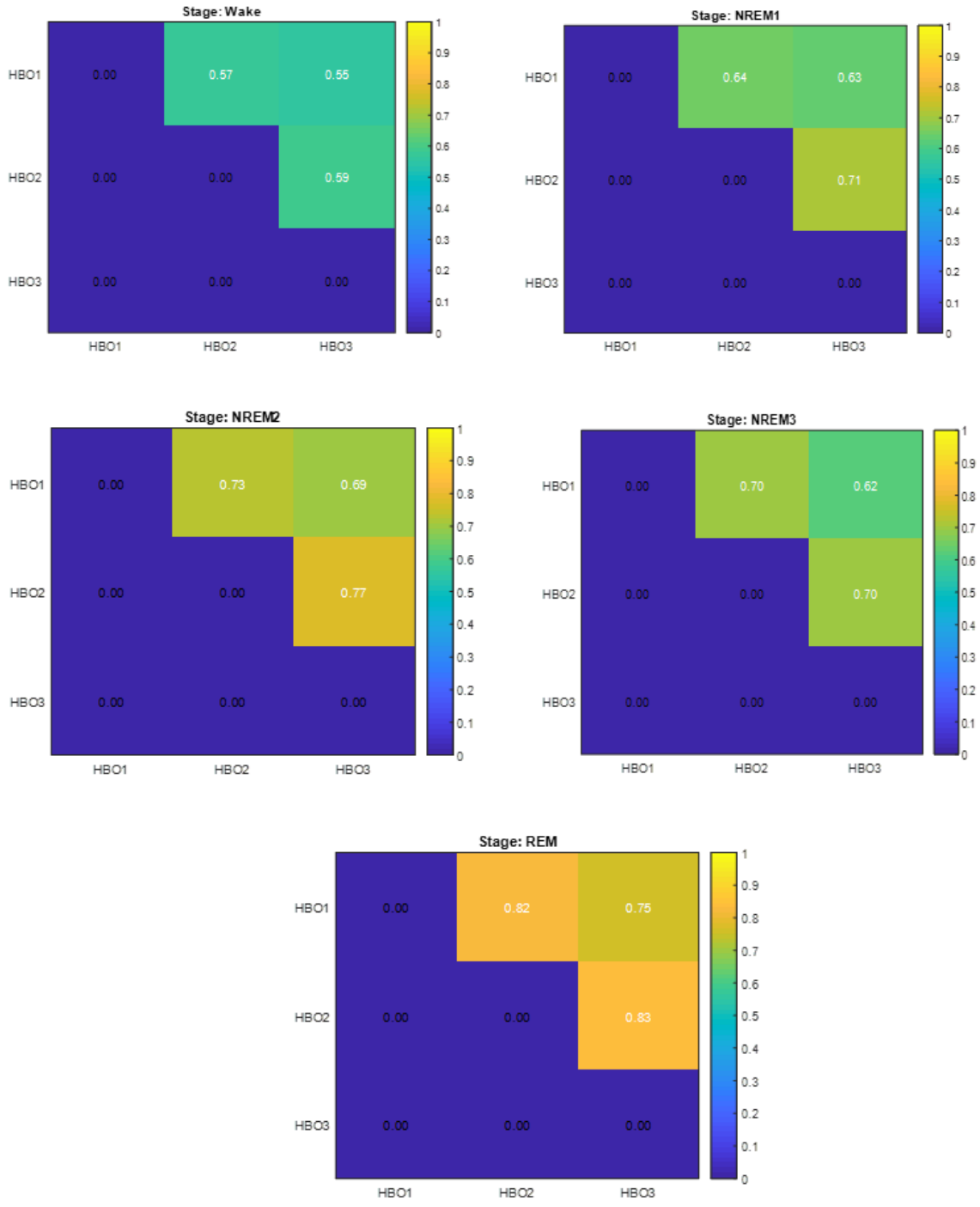

Figure 34: Connectivity matrices for cross correlation among HBO channels

The ANOVA test showed p-value 0.0059 which is less than the significance level indicating that there are some differences in the means of the groups. Connectivity is highest in NREM2 stage and least in wake.

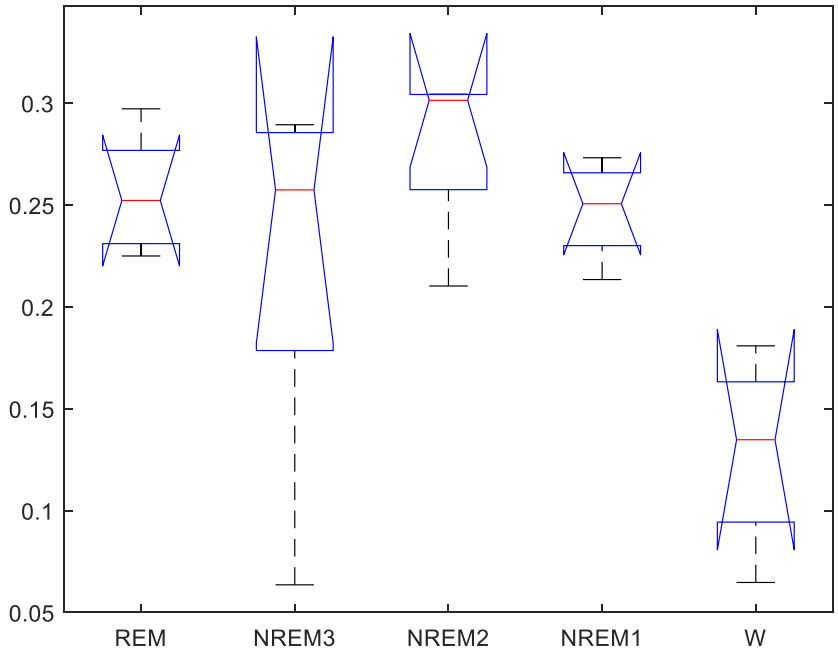

Source	SS	df	MS	F	Prob>F
Groups	0.05786	4	0.01446	5.08	0.0059
Error	0.05408	19	0.00285		
Total	0.11194	23			

Figure 35: ANOVA results for cross correlation among HBO channels in different sleep stages

Hereafter, a post-hoc t-test was carried out to compare the means of different groups. It showed that the mean connectivity is significantly less in wake stage than that in REM, NREM2 and NREM1 stage. Thus, the difference in connectivtiy between HBO channels during wake, NREM and REM sleep is statistically significant.

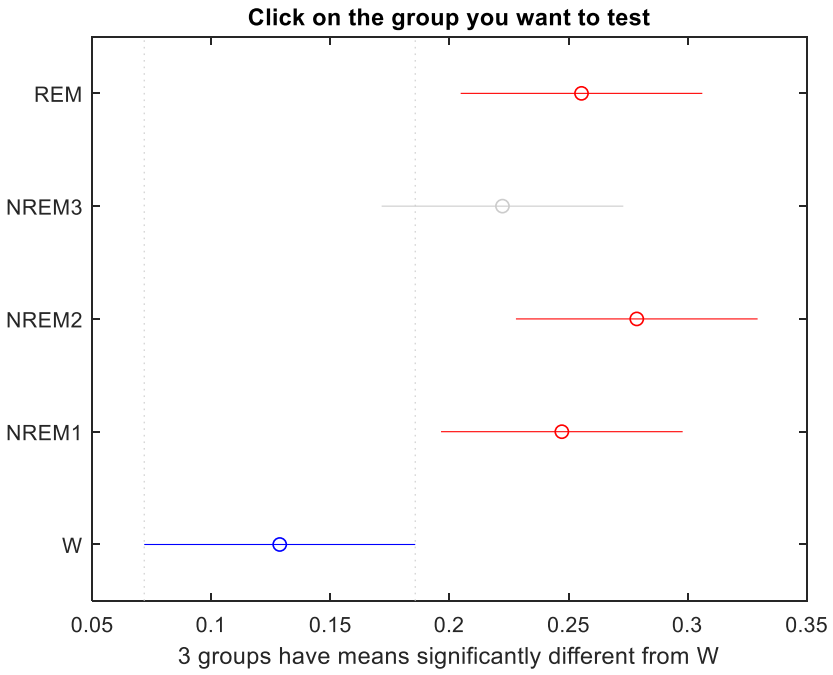

Figure 36: Multiple comparison test showing connectivity wake stage to be significantly different from NREM1, NREM2, REM

5.2Cross-correlation between de-oxyhemoglobin (HHB) channels

The measures derived from HHB channels agreed with that derived from HBO channels showing increased connectivity from wake stage to NREM2 stage until it decreased in NREM3 stage (figure 37).

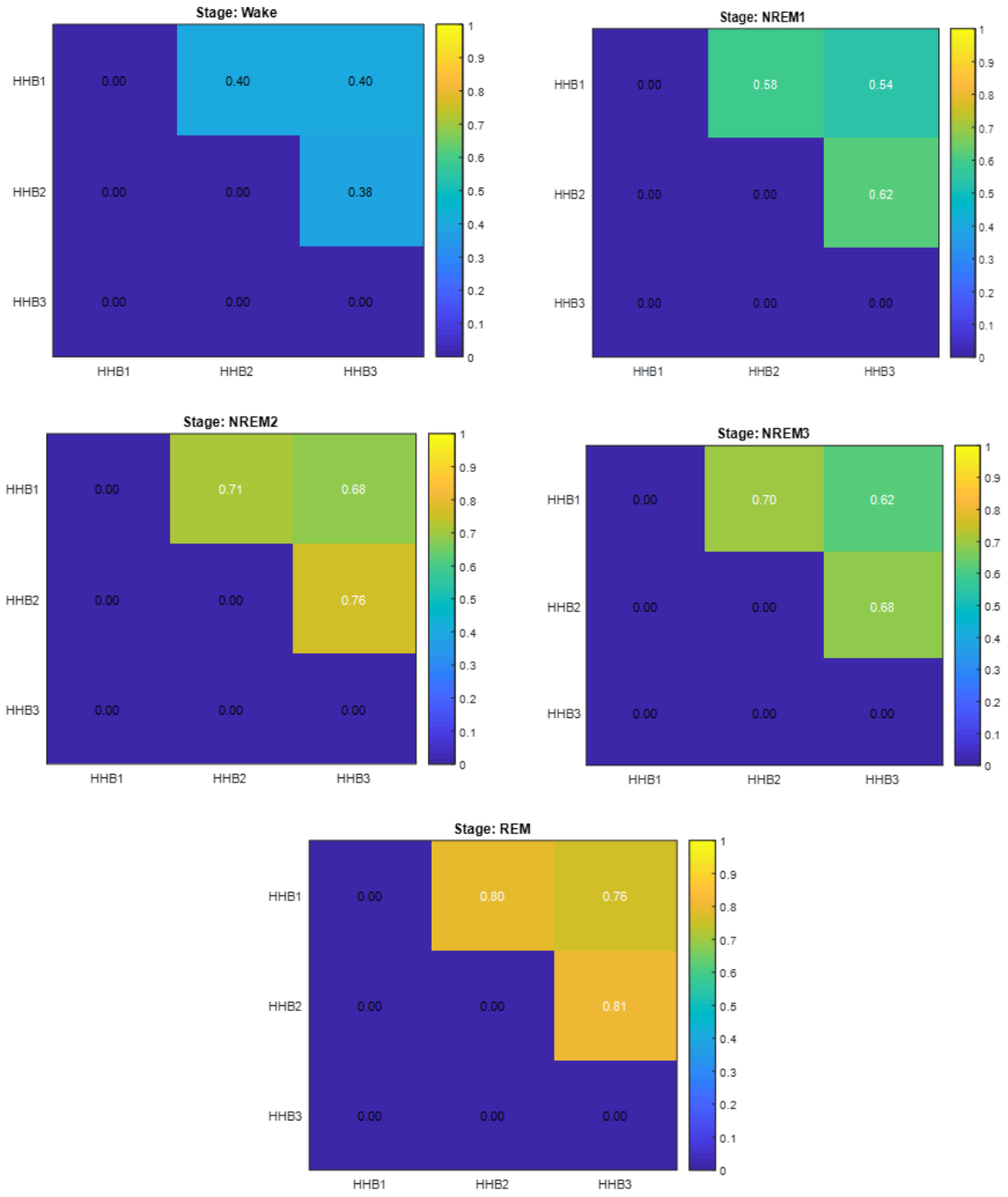

Figure 37: Connectivity matrices for cross correlation among HHB channels during different sleep stages

ANOVA test was significant with p-value of 0.0403 and post hoc t-test showed that the mean connectivity during NREM2 stage is significantly greater than that in wakefulness.

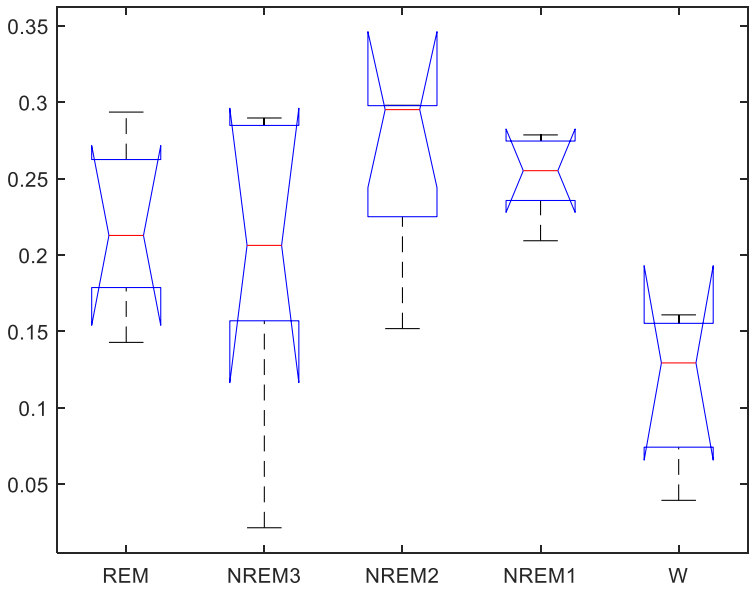

Source	SS	df	MS	F	Prob>F
Groups	0.05753	4	0.01438	3.1	0.0403
Error	0.08819	19	0.00464		
Total	0.14573	23			

Figure 38: ANOVA results for cross-correlation among HHB channels in different sleep stages

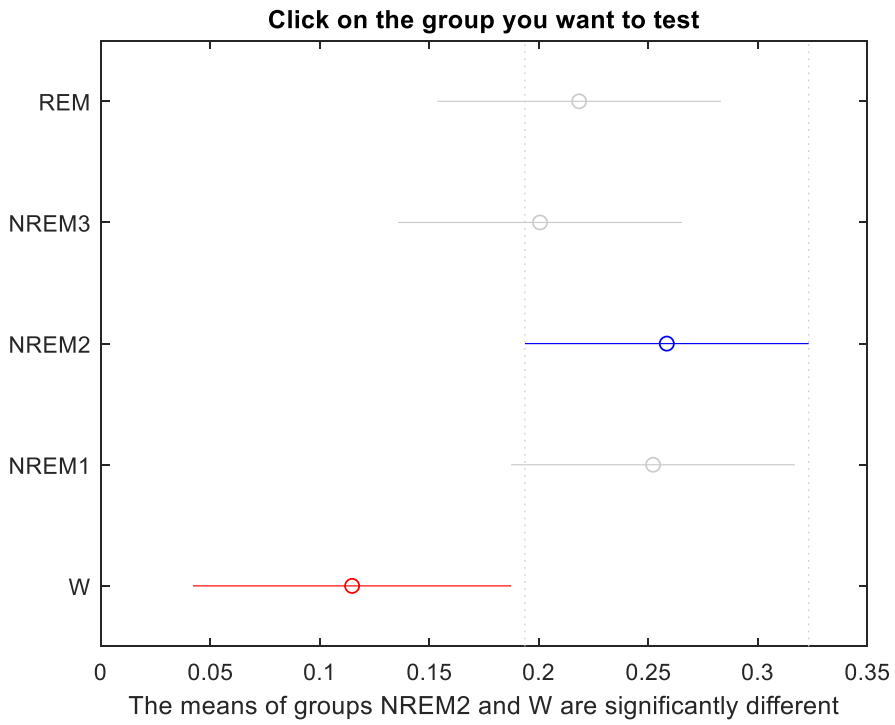

Figure 39: Multiple comparison test for cross correlation between HHB channels

5.3 Cross-correlation between HBO and HHB

The cross-correlation measure between HBO and HHB channels showed anti-correlated signals at all stage. This is an indication that when concentration of HBO increases, HHB decreases and vice versa. Tong et al., (2011) provide similar suggestion for their finding on anti-correlated HBO and HHB signals [112].

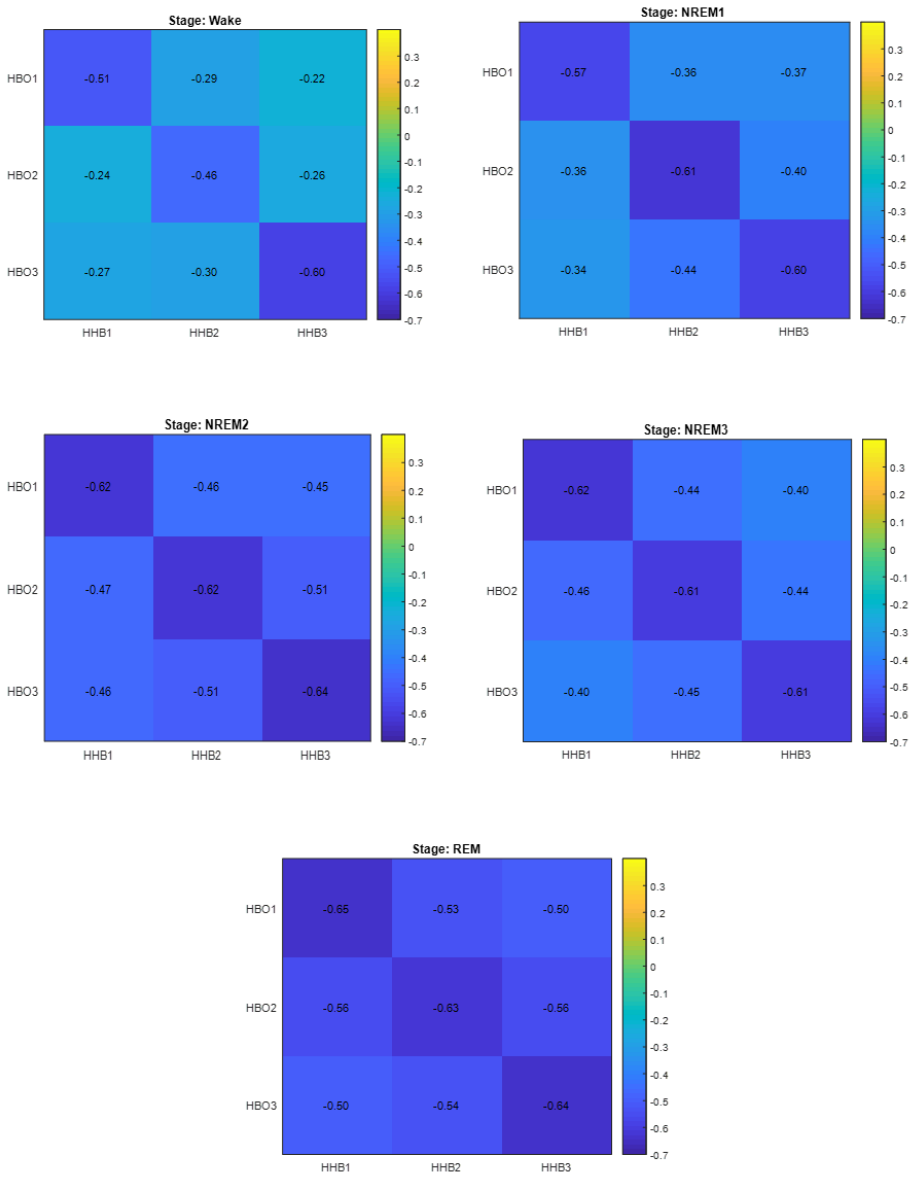

Figure 40: Connectivity matrices for cross correlation between HBO and HHB channels during different sleep stages

The ANOVA test showed p-value 0.0355 which was significant and hence a post hoc t-test was carried out which showed that stages NREM2 and wake had significant difference in their mean connectivity, the former with higher negative correlation.

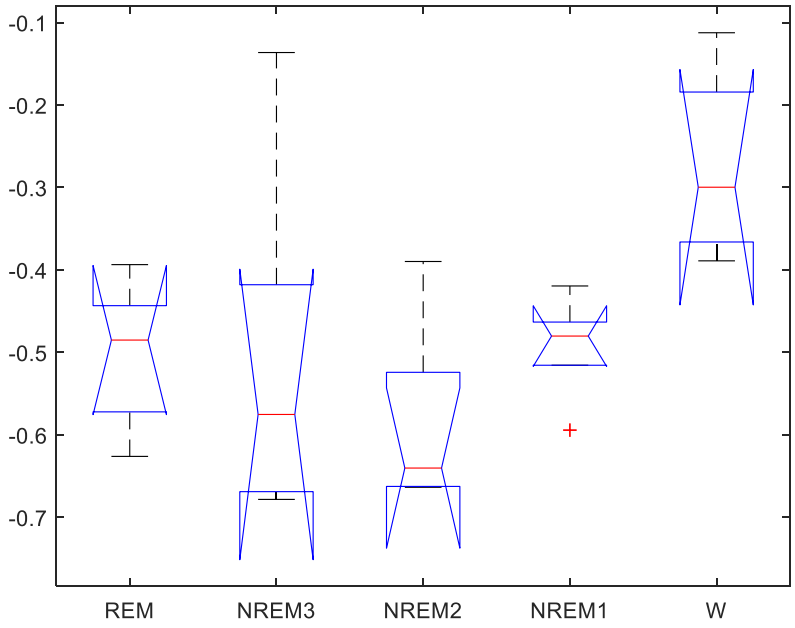

Source	SS	df	MS	F	Prob>F
Groups	0.23192	4	0.05798	3.22	0.0355
Error	0.34239	19	0.01802		
Total	0.57431	23			

Figure 41: ANOVA results for cross-correlation between HBO and HHB channels during different sleep stages

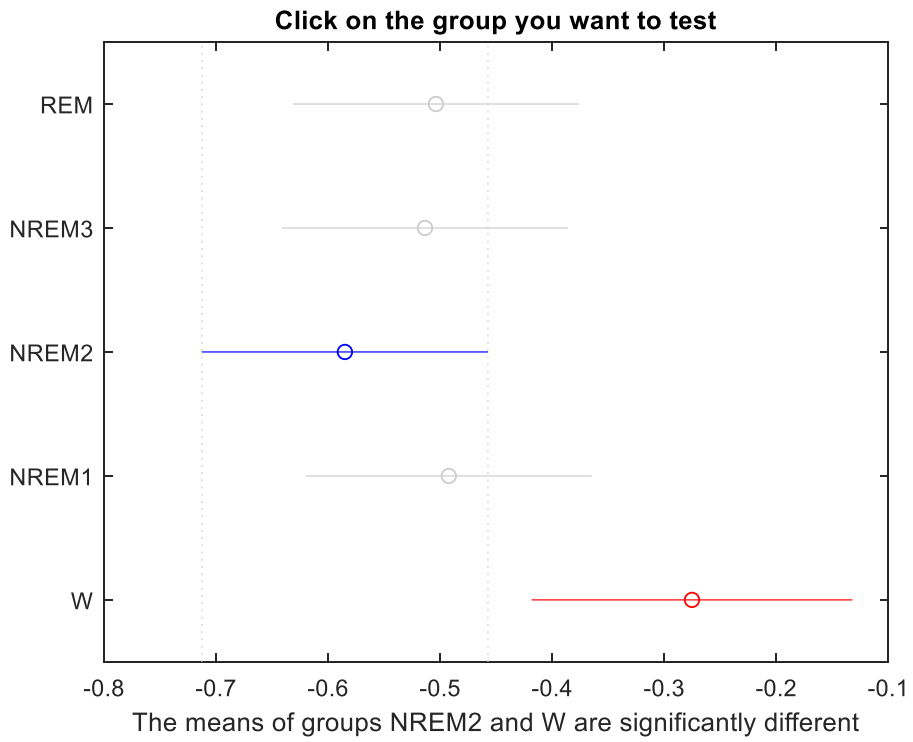

Figure 42: Multiple comparison test for cross correlation between HBO and HHB channels

The findings from cross correlation between NIRS channels suggest that there exist statistically significant differences between connectivity during wake and NREM2 stage for all NIRS channel derivations. Also, HBO derivations show difference in connectivity during wake stage from NREM and REM sleep. Above all, highest correlation between HBO channels and also between HHB channels exist during NREM2 stage and the least during wake.

5.4 Discussion

5.4.1 Functional connectivity in prefrontal region: A cross-correlation measure

As obtained from the cross-correlation measure for averaged connectivity between NIRS channels, it was observed that brain functional connectivity first increases from wake to NREM1 and NREM2, and then decreases in NREM3 stage of sleep as sleep progresses. We are unable to directly compare this finding with that in literature directly because they either involve other

modalities like EEG and MRI, or exclude NREM3 stage of sleep, or only focus on hemodynamic changes rather than brain connectivity [85, 113]. Nevertheless, the finding is somewhat similar to the one by Horovitz et al., (2009) and Sämann et al., (2011) who depicted reduced brain connectivity in the prefrontal region during slow wave sleep using functional MRI [114, 115].

Also, functional connectivity of occipital region with frontal and central brain regions increase during REM sleep as indicated by the adjajency matrix. This finding could account for the increased eye movements in REM sleep because of the activation of visual cortex located in the occipital region. Igawa et al., (2001) found an increase in oxyhemoglobin concentration in the visual cortex during REM sleep and suggested that this could also explain the intense dreaming activities at this stage of sleep [116].

5.4.2 Hemodynamic changes during sleep

The decrease in cross-correlation measure between NIRS channels in NREM3 stage can correspond to reduced cerebral hemodynamic activity in this particular stage as per Nasi et al., (2011) where they showed prevalence of reduced spontaneous, slow hemodynamic oscillations in the slow wave sleep [85]. This leads to an inference that reduced hemodynamic activity in the prefrontal cortex is accompanied by reduced hemodynamic activity itself. Furthermore, this inference can also put an insight to the fact that a person is difficult to awaken when he is in deep or NREM3 sleep due to reduced hemodynamic activity and prefrontal connectivity during NREM3 stage of sleep.

Also, the increased connectivity in REM stage can account for the fact that there is increased hemodynamic activity during REM sleep in the activated dorsolateral pre-frontal cortex as compared to that in slow wave sleep [85, 117]. Kubota et al., (2011) also suggested that the

increased hemodynamic activity might also account for the role of REM sleep in cognitive functions [117].

Chapter 6 : Conclusion

The exploration of sleep science needs a rigorous tool able to provide important physiological details such as oxygenation and electric activity throughout sleep. While most of the researches with NIRS have been targeted towards finding out the cerebral oxygenation and concentration changes, the understanding of connectivity changes in relation to electrophysiology and hemodynamic during a whole night sleep study has yet not been explored. Moreover, the possible relation between cerebral oxygenation changes and electrical activities during these sleep stages remains unexplored.

As found in this research, the significant difference in connectivity along right prefrontal cortex and left occipital using NIRS and EEG signals, as well as that in the right prefrontal cortex using only NIRS, across the different sleep stages suggests that measure of connectivity can be a useful tool in classifying sleep stages as well as in understanding phenomenon of sleep. Moreover, the connectivity networks derived from the measure can provide supporting evidence to researches so far in the field of sleep and sleep medicine. Further research with brain connectivity during whole night sleep can provide valuable information on cerebral mechanisms.

Chapter 7 : Limitations and recommendations

Although the research outcome provides an insight into the potential of brain connectivity measures in defining sleep phenomenon, there are certain limitations. Firstly, the sample size is limited to 5 subjects, thus giving us a small dataset. Secondly, the process of synchronisation between PSG and NIRS data is not automatic and digital, but rather manual. It is recommended that the study be carried out with some robust synchronisation tools so that the outcomes are more precise. Furthermore, the location of NIRS sensors used in the research for head plot of connectivity across channels is approximate. The results can be better demonstrated with precise location of the three transmitters.

The research uses only two measures of connectivity, while there are multiple options available. Reproduction of the research outcomes could be done by changing these measures as well. The fact that connectivity measures are affected by the choice of EEG electrode reference point forms another consideration to be done in reproduction of the research results as it can be redone by choosing reference electrodes more deliberately to avoid chances of bias caused by reference issues.

Chapter 8 : Author's Contribution

The author's primary role has been in developing the protocol for data acquisition, screening and setting subjects up for data collection and monitoring them whole night, cleaning and preparing the signals for further processing, designing experiments to obtain meaningful results and finally analysing the connectivity outcomes. The MATLAB codes for data processing and connectivity measures were primarily written by A / P Kenneth Pope and Hanieh Bakhshayesh, while they were edited and modified as required for the project by the author. Previous work in this field by them has been limited to functional connectivity measures using EEG only while this research focuses on effective connectivity with additional NIRS signals.

Chapter 9 : References

1. Aminoff, M.J., Boller, F. and Swaab, D.F., 2011. We spend about one-third of our life either sleeping or attempting to do so. *Handbook of clinical neurology*, *98*, pp.vii.
2. Hillman, D.R., Murphy, A.S., Antic, R. and Pezzullo, L., 2006. The economic cost of sleep disorders. *Sleep*, *29*(3), pp.299-305.
3. Hedner, J., White, D.P., Malhotra, A., Herscovici, S., Pittman, S.D., Zou, D., Grote, L. and Pillar, G., 2011. Sleep staging based on autonomic signals: a multi-center validation study. *Journal of clinical sleep medicine*, *7*(03), pp.301-306.
4. Hsu, Y.L., Yang, Y.T., Wang, J.S. and Hsu, C.Y., 2013. Automatic sleep stage recurrent neural classifier using energy features of EEG signals. *Neurocomputing*, *104*, pp.105-114.
5. Tagliazucchi, E., von Wegner, F., Morzelewski, A., Borisov, S., Jahnke, K. and Laufs, H., 2012. Automatic sleep staging using fMRI functional connectivity data. *Neuroimage*, *63*(1), pp.63-72.
6. Sporns, O., Chialvo, D.R., Kaiser, M. and Hilgetag, C.C., 2004. Organization, development and function of complex brain networks. *Trends in cognitive sciences*, *8*(9), pp.418-425.
7. Raichle, M.E., 1998. Behind the scenes of functional brain imaging: a historical and physiological perspective. *Proceedings of the National Academy of Sciences*, *95*(3), pp.765-772.
8. Sakkalis, V., 2011. Review of advanced techniques for the estimation of brain connectivity measured with EEG/MEG. *Computers in biology and medicine*, *41*(12), pp.1110-1117.

9. Bakhshayesh, H., Fitzgibbon, S.P. and Pope, K.J., 2014, December. A comparative study of the detection of direct causal influence with bivariate and multivariate measures for EEG. In *2014 IEEE Conference on Biomedical Engineering and Sciences (IECBES)* (pp. 719-723).
10. Friston, K.J., Jezzard, P. and Turner, R., 1994. Analysis of functional MRI time-series. *Human brain mapping*, *1*(2), pp.153-171.
11. Razak, F.A. and Jensen, H.J., 2014. Quantifying 'causality' in complex systems: understanding transfer entropy. *PLoS One*, *9*(6), p.e99462.
12. Friston, K.J., 2011. Functional and effective connectivity: a review. *Brain connectivity*, *1*(1), pp.13-36.
13. Friston, K.J., 1994. Functional and effective connectivity in neuroimaging: a synthesis. *Human brain mapping*, *2*(1-2), pp.56-78.
14. Jirsa, V.K. and Haken, H., 1997. A derivation of a macroscopic field theory of the brain from the quasi-microscopic neural dynamics. *Physica D: Nonlinear Phenomena*, *99*(4), pp.503-526.
15. Lang, E.W., Tomé, A.M., Keck, I.R., Górriz-Sáez, J.M. and Puntonet, C.G., 2012. Brain connectivity analysis: a short survey. *Computational intelligence and neuroscience*, *2012*, p.8.
16. Friston, K.J., Frith, C.D., Liddle, P.F. and Frackowiak, R.S.J., 1993. Functional connectivity: the principal-component analysis of large (PET) data sets. *Journal of Cerebral Blood Flow & Metabolism*, *13*(1), pp.5-14.
17. Wiener, N., 1956. The theory of prediction. *Modern mathematics for engineers*.

18. Schuster, H.G. ed., 2008. *Reviews of nonlinear dynamics and complexity*. Weinheim: Wiley-VCH.

19. Rubinov, M. and Sporns, O., 2010. Complex network measures of brain connectivity: uses and interpretations. *Neuroimage*, *52*(3), pp.1059-1069.

20. Pessoa, L., 2014. Understanding brain networks and brain organization. *Physics of life reviews*, *11*(3), pp.400-435.

21. Khalil, M.I., 2013. Accelerating cross-correlation applications via parallel computing. *International Journal of Image, Graphics and Signal Processing*, *5*(12), p.26.

22. Ding, M., Chen, Y. and Bressler, S.L., 2006. Granger causality: basic theory and application to neuroscience. *Handbook of time series analysis: recent theoretical developments and applications*, pp.437-460.

23. Biswal, B., Zerrin Yetkin, F., Haughton, V.M. and Hyde, J.S., 1995. Functional connectivity in the motor cortex of resting human brain using echo-planar MRI. *Magnetic resonance in medicine*, *34*(4), pp.537-541.

24. O'reilly, J.X., Woolrich, M.W., Behrens, T.E., Smith, S.M. and Johansen-Berg, H., 2012. Tools of the trade: psychophysiological interactions and functional connectivity. *Social cognitive and affective neuroscience*, *7*(5), pp.604-609.

25. Bendat, J.S. and Piersol, A.G., 2011. *Random data: analysis and measurement procedures* (Vol. 729). John Wiley & Sons.

26. Liao, W., Mantini, D., Zhang, Z., Pan, Z., Ding, J., Gong, Q., Yang, Y. and Chen, H., 2010. Evaluating the effective connectivity of resting state networks using conditional Granger causality. *Biological cybernetics*, *102*(1), pp.57-69.

27. Friston, K., 2009. Causal modelling and brain connectivity in functional magnetic resonance imaging. *PLoS biology*, *7*(2).

28. Friston, K., 2011. Dynamic causal modeling and Granger causality Comments on: The identification of interacting networks in the brain using fMRI: Model selection, causality and deconvolution. *Neuroimage*, *58*(2-2), p.303.

29. Geweke, J.F., 1984. Measures of conditional linear dependence and feedback between time series. *Journal of the American Statistical Association*, *79*(388), pp.907-915.

30. Chen, Y., Bressler, S.L. and Ding, M., 2006. Frequency decomposition of conditional Granger causality and application to multivariate neural field potential data. *Journal of neuroscience methods*, *150*(2), pp.228-237.

31. Papana, A., Kugiumtzis, D. and Larsson, P.G., 2011. Reducing the bias of causality measures. *Physical Review E*, *83*(3), p.036207.

32. Kamiński M, Ding M, Truccolo WA, Bressler SL. Evaluating causal relations in neural systems: Granger causality, directed transfer function and statistical assessment of significance. Biological cybernetics. 2001 Aug 1;85(2):145-57.

33. Blinowska, K.J. and Kamiński, M., 2006. 15 Multivariate Signal Analysis by Parametric Models. *Handbook of Time Series Analysis: Recent Theoretical Developments and Applications*, p.373.

34. Kaminski, M.J. and Blinowska, K.J., 1991. A new method of the description of the information flow in the brain structures. *Biological cybernetics*, *65*(3), pp.203-210.

35. Baccalá, L.A. and Sameshima, K., 2001. Partial directed coherence: a new concept in neural structure determination. *Biological cybernetics*, *84*(6), pp.463-474.

36. Lachaux, J.P., Rodriguez, E., Martinerie, J. and Varela, F.J., 1999. Measuring phase synchrony in brain signals. *Human brain mapping*, *8*(4), pp.194-208.

37. Shannon, C.E., 1948. A mathematical theory of communication. *Bell system technical journal*, *27*(3), pp.379-423.

38. Timme, N.M. and Lapish, C., 2018. A Tutorial for Information Theory in Neuroscience. *eNeuro*, *5*(3).

39. Kullback S., 1997. Information theory and statistics. Courier Corporation.

40. Dodonova, Y., Korolev, S., Tkachev, A., Petrov, D., Zhukov, L. and Belyaev, M., 2016, September. Classification of structural brain networks based on information divergence of graph spectra. In *2016 IEEE 26th International Workshop on Machine Learning for Signal Processing (MLSP)* (pp. 1-6). IEEE.

41. Mars RB, Sotiropoulos SN, Passingham RE, Sallet J, Verhagen L, Khrapitchev AA, Sibson N, Jbabdi S. 2018. Whole brain comparative anatomy using connectivity blueprints. Elife.

42. Shao S, Guo C, Luk W, Weston S. 2014. Accelerating transfer entropy computation. In International Conference on Field-Programmable Technology (FPT), pp.60-67. IEEE.

43. Cerf NJ, Adami C. 1999. Quantum extension of conditional probability. Physical Review A, 60(2):893.

44. Shovon, M.H.I., Nandagopal, N., Vijayalakshmi, R., Du, J.T. and Cocks, B., 2017. Directed connectivity analysis of functional brain networks during cognitive activity using transfer entropy. *Neural Processing Letters*, *45*(3), pp.807-824.

45. Schreiber T. Measuring information transfer. Physical review letters. 2000 Jul 10;85(2):461.

46. Vakorin, V.A., Kovacevic, N. and McIntosh, A.R., 2010. Exploring transient transfer entropy based on a group-wise ICA decomposition of EEG data. *Neuroimage*, *49*(2), pp.1593-1600.

47. Paluš, M., Komárek, V., Hrnčíř, Z. and Štěrbová, K., 2001. Synchronization as adjustment of information rates: detection from bivariate time series. *Physical Review E*, *63*(4), p.046211.

48. Sabesan, S., Good, L.B., Tsakalis, K.S., Spanias, A., Treiman, D.M. and Iasemidis, L.D., 2009. Information flow and application to epileptogenic focus localization from intracranial EEG. *IEEE Transactions on neural systems and rehabilitation engineering*, *17*(3), pp.244-253.

49. Garofalo, M., Nieus, T., Massobrio, P. and Martinoia, S., 2009. Evaluation of the performance of information theory-based methods and cross-correlation to estimate the functional connectivity in cortical networks. *PloS one*, *4*(8), p.e6482.

50. Vicente R, Wibral M, Lindner M, Pipa G. Transfer entropy—a model-free measure of effective connectivity for the neurosciences. Journal of computational neuroscience. 2011 Feb 1;30(1):45-67.

51. Faes, L., Marinazzo, D., Jurysta, F. and Nollo, G., 2015. Linear and non-linear brain–heart and brain–brain interactions during sleep. *Physiological measurement*, *36*(4), p.683.

52. Swadlow HA, Waxman SG. Axonal conduction delays. Scholarpedia. 2012 Jun 5;7(6):1451.

53. Gharib, S., Sutherling, W.W., Nakasato, N., Barth, D.S., Baumgartner, C., Alexopoulos, N., Taylor, S. and Rogers, R.L., 1995. MEG and ECoG localization

accuracy test. *Electroencephalography and clinical neurophysiology*, *94*(2), pp.109-114.

54. Melek, H., Gunluoglu, M.Z., Demir, A., Akin, H., Olcmen, A. and Dincer, S.I., 2008. Role of positron emission tomography in mediastinal lymphatic staging of non-small cell lung cancer. *European Journal of Cardio-Thoracic Surgery*, *33*(2), pp.294-299.
55. Kidwell, C.S. and Hsia, A.W., 2006. Imaging of the brain and cerebral vasculature in patients with suspected stroke: advantages and disadvantages of CT and MRI. *Current neurology and neuroscience reports*, *6*(1), pp.9-16.
56. Williams D, Ludbrook G. 2003. Transcranial doppler ultrasound. Australasian Anaesthesia:127
57. Sheppard, N., Willis, H.A. and Rigg, J.C., 1985. Names, symbols, definitions and units of quantities in optical spectroscopy (Recommendations 1984). *Pure and Applied Chemistry*, *57*(1), pp.105-120.
58. Jasper, H.H., 1958. The ten-twenty electrode system of the International Federation. *Electroencephalogr. Clin. Neurophysiol.*, *10*, pp.370-375.
59. Lau, T.M., Gwin, J.T. and Ferris, D.P., 2012. How many electrodes are really needed for EEG-based mobile brain imaging? *Journal of Behavioral and Brain Science*, *2*(03), p.387.
60. Pizza, F., Biallas, M., Wolf, M., Werth, E. and Bassetti, C.L., 2010. Nocturnal cerebral hemodynamics in snorers and in patients with obstructive sleep apnea: a near-infrared spectroscopy study. *Sleep*, *33*(2), pp.205-210.
61. Zhan, Y., Eggebrecht, A.T., Culver, J.P. and Dehghani, H., 2012. Singular value decomposition-based regularization prior to spectral mixing improves crosstalk in

dynamic imaging using spectral diffuse optical tomography. *Biomedical optics express*, *3*(9), pp.2036-2049.

62. Delpy, D.T., Cope, M., van der Zee, P., Arridge, S.R., Wray, S. and Wyatt, J.S., 1988. Estimation of optical pathlength through tissue from direct time of flight measurement. *Physics in Medicine & Biology*, *33*(12), p.1433.
63. Manual Portalite FOR OXYSOFT 3.0.89 and higher and POTRASOFT 2.0.8.214 and higher, 2014.*User Manual, Artinis Medical System, Einsteinweg, The Netherlands*.
64. Abdelnour, A.F. and Huppert, T., 2009. Real-time imaging of human brain function by near-infrared spectroscopy using an adaptive general linear model. *Neuroimage*, *46*(1), pp.133-143.
65. Fekete, T., Rubin, D., Carlson, J.M. and Mujica-Parodi, L.R., 2011. The NIRS analysis package: noise reduction and statistical inference. *PloS one*, *6*(9), p.e24322.
66. Utsugi, K., Obata, A., Sato, H., Katsura, T., Sagara, K., Maki, A. and Koizumi, H., 2007, August. Development of an optical brain-machine interface. In *2007 29th Annual International Conference of the IEEE Engineering in Medicine and Biology Society* (pp. 5338-5341). IEEE.
67. Cui, X., Bray, S. and Reiss, A.L., 2010. Functional near infrared spectroscopy (NIRS) signal improvement based on negative correlation between oxygenated and deoxygenated hemoglobin dynamics. *Neuroimage*, *49*(4), pp.3039-3046.
68. Kleitman, N., 1963. *Sleep and wakefulness*. University of Chicago Press.
69. "Sleep-wake cycle: its physiology and impact on health"*(PDF). National Sleep Foundation. 2006. Retrieved 24 May 2017.*

70. Carskadon, M.A., & Dement, W.C. (2011). Monitoring and staging human sleep. In M.H. Kryger, T. Roth, & W.C. Dement (Eds.), Principles and practice of sleep medicine, 5th edition, (pp 16-26). St. Louis: Elsevier Saunders

71. Berry, R.B., Brooks, R., Gamaldo, C.E., Harding, S.M., Marcus, C.L. and Vaughn, B.V., 2012. The AASM manual for the scoring of sleep and associated events. *Rules, Terminology and Technical Specifications, Darien, Illinois, American Academy of Sleep Medicine*.

72. Berry, R.B., 2011. *Fundamentals of Sleep Medicine E-Book*. Elsevier Health Sciences.

73. Šušmáková, K., 2004. Human sleep and sleep EEG. *Measurement science review*, *4*(2), pp.59-74.

74. Altevogt, B.M. and Colten, H.R. eds., 2006. *Sleep disorders and sleep deprivation: an unmet public health problem*. National Academies Press.

75. Hillman, D.R., Murphy, A.S., Antic, R. and Pezzullo, L., 2006. The economic cost of sleep disorders. *Sleep*, *29*(3), pp.299-305.

76. Jafari, B. and Mohsenin, V., 2010. Polysomnography. *Clinics in chest medicine*, *31*(2), pp.287-297.

77. Jobsis, F.F., 1977. Noninvasive, infrared monitoring of cerebral and myocardial oxygen sufficiency and circulatory parameters. *Science*, *198*(4323), pp.1264-1267.

78. Brazy, J.E., Lewis, D.V., Mitnick, M.H. and vander Vliet, F.F.J., 1985. Noninvasive monitoring of cerebral oxygenation in preterm infants: preliminary observations. *Pediatrics*, *75*(2), pp.217-225.

79. Ferrari, M., Zanette, E., Sideri, G., Giannini, I., Fieschi, C. and Carpi, A., 1987. Effects of carotid compression, as assessed by near infrared spectroscopy, upon cerebral blood

volume and haemoglobin oxygen saturation. *Journal of the Royal Society of Medicine*, *80*(2), pp.83-87.

80. Zabel, T.A. and Chute, D.L., 2002. Educational neuroimaging: A proposed neuropsychological application of near-infrared spectroscopy (nIRS). *The Journal of head trauma rehabilitation*, *17*(5), pp.477-488.
81. Valipour, A., McGown, A.D., Makker, H., O'sullivan, C. and Spiro, S.G., 2002. Some factors affecting cerebral tissue saturation during obstructive sleep apnoea. *European Respiratory Journal*, *20*(2), pp.444-450.
82. McTiernan, K.B., Garnett, M.H., Mauquoy, D., Ineson, P. and Coûteaux, M.M., 1998. Use of near-infrared reflectance spectroscopy (NIRS) in palaeoecological studies of peat. *The Holocene*, *8*(6), pp.729-740.
83. Cui, X., Bray, S., Bryant, D.M., Glover, G.H. and Reiss, A.L., 2011. A quantitative comparison of NIRS and fMRI across multiple cognitive tasks. *Neuroimage*, *54*(4), pp.2808-2821.
84. Wallois, F., Mahmoudzadeh, M., Patil, A. and Grebe, R., 2012. Usefulness of simultaneous EEG–NIRS recording in language studies. *Brain and language*, *121*(2), pp.110-123.
85. Näsi, T., Virtanen, J., Noponen, T., Toppila, J., Salmi, T. and Ilmoniemi, R.J., 2011. Spontaneous hemodynamic oscillations during human sleep and sleep stage transitions characterized with near-infrared spectroscopy. *PLoS One*, *6*(10), p.e25415.
86. Hayakawa, T., Terashima, M., Kayukawa, Y., Ohta, T. and Okada, T., 1996. Changes in cerebral oxygenation and hemodynamics during obstructive sleep apneas. *Chest*, *109*(4), pp.916-921.

87. Spielman, A.J., Zhang, G., Yang, C.M., D'Ambrosio, P., Serizawa, S., Nagata, M., von Gizycki, H. and Alfano, R.R., 2000. Intracerebral hemodynamics probed by near infrared spectroscopy in the transition between wakefulness and sleep. *Brain research*, *866*(1-2), pp.313-325.

88. Münger, D.M., Bucher, H.U. and Duc, G., 1998. Sleep state changes associated with cerebral blood volume changes in healthy term newborn infants. *Early human development*, *52*(1), pp.27-42.

89. Onoe, H., Watanabe, Y., Tamura, M. and Hayaishi, O., 1991. REM sleep-associated hemoglobin oxygenation in the monkey forebrain studied using near-infrared spectrophotometry. *Neuroscience letters*, *129*(2), pp.209-213.

90. Wallois, F., Mahmoudzadeh, M., Patil, A. and Grebe, R., 2012. Usefulness of simultaneous EEG–NIRS recording in language studies. *Brain and language*, *121*(2), pp.110-123.

91. Roche-Labarbe, N., Zaaimi, B., Berquin, P., Nehlig, A., Grebe, R. and Wallois, F., 2008. NIRS-measured oxy-and deoxyhemoglobin changes associated with EEG spike-and-wave discharges in children. *Epilepsia*, *49*(11), pp.1871-1880.

92. Nguyen, T., Ahn, S., Jang, H., Jun, S.C. and Kim, J.G., 2017. Utilization of a combined EEG/NIRS system to predict driver drowsiness. *Scientific reports*, *7*, p.43933.

93. Liu, Y., Ayaz, H., Curtin, A., Onaral, B. and Shewokis, P.A., 2013, July. Towards a hybrid P300-based BCI using simultaneous fNIR and EEG. In *International Conference on Augmented Cognition* (pp. 335-344). Springer, Berlin, Heidelberg.

94. Balconi, M., Grippa, E. and Vanutelli, M.E., 2015. What hemodynamic (fNIRS), electrophysiological (EEG) and autonomic integrated measures can tell us about emotional processing. *Brain and cognition*, *95*, pp.67-76.

95. National Health and Medical Research Council (Australia), 2007. *National statement on ethical conduct in human research*. National Health and Medical Research Council.

96. Johns, M.W., 1991. A new method for measuring daytime sleepiness: the Epworth sleepiness scale. *Sleep*, *14*(6), pp.540-545.

97. Buysse, D.J., Reynolds III, C.F., Monk, T.H., Berman, S.R. and Kupfer, D.J., 1989. The Pittsburgh Sleep Quality Index: a new instrument for psychiatric practice and research. *Psychiatry research*, *28*(2), pp.193-213.

98. Makeig, S., Westerfield, M., Jung, T.P., Enghoff, S., Townsend, J., Courchesne, E. and Sejnowski, T.J., 2002. Dynamic brain sources of visual evoked responses. *Science*, *295*(5555), pp.690-694.

99. Palaniappan, R., 2011. *Biological signal analysis*. BookBoon.

100. Hilton, A. and Armstrong, R.A., 2006. Statnote 6: post-hoc ANOVA tests.

101. Good, P., 2013. *Permutation tests: a practical guide to resampling methods for testing hypotheses*. Springer Science & Business Media.

102. Tagliazucchi, E. and Laufs, H., 2014. Decoding wakefulness levels from typical fMRI resting-state data reveals reliable drifts between wakefulness and sleep. *Neuron*, *82*(3), pp.695-708.

103. Mak-McCully, R.A., Rolland, M., Sargsyan, A., Gonzalez, C., Magnin, M., Chauvel, P., Rey, M., Bastuji, H. and Halgren, E., 2017. Coordination of cortical and

thalamic activity during non-REM sleep in humans. *Nature communications*, *8*, p.15499.

104. Steriade, M., 2003.*Frontiers in bioscience*, *8*, pp.878-899.

105. Massimini, M., Huber, R., Ferrarelli, F., Hill, S. and Tononi, G., 2004. The sleep slow oscillation as a traveling wave. *Journal of Neuroscience*, *24*(31), pp.6862-6870.

106. Krone, L., Frase, L., Piosczyk, H., Selhausen, P., Zittel, S., Jahn, F., Kuhn, M., Feige, B., Mainberger, F., Klöppel, S. and Riemann, D., 2017. Top-down control of arousal and sleep: Fundamentals and clinical implications. *Sleep medicine reviews*, *31*, pp.17-24.

107. Jones, B.E., 2003. Arousal systems. *Front Biosci*, *8*(5), pp.438-51.

108. Migliorelli, C., Bachiller, A., Andrade, A.G., Alonso, J.F., Mañanas, M.A., Borja, C., Giménez, S., Antonijoan, R.M., Varga, A.W., Osorio, R.S. and Romero, S., 2019. Alterations in EEG connectivity in healthy young adults provide an indicator of sleep depth. *Sleep*.

109. Jurysta, F., Marinazzo, D. and Linkowski, P., 2012. Functional and Effective Connectivity in Healthy Human EEG across Sleep Stages. In *Belgian Brain Council 2012*.

110. ‘Nerve conduction velocity’. 2019. *Wikipedia*. Available at https://en.wikipedia.org/wiki/Nerve_conduction_velocity#cite_note-Hopkins_NCS-8 (Accessed: 4 May 2019).

111. Fischer, A.Q., Taormina, M.A., Akhtar, B. and Chaudhary, B.A., 1991. The effect of sleep on intracranial hemodynamics: a transcranial Doppler study. *Journal of child neurology*, *6*(2), pp.155-158.

112. Tong, Y., Hocke, L.M. and Frederick, B.B., 2011. Isolating the sources of widespread physiological fluctuations in functional near-infrared spectroscopy signals. *Journal of biomedical optics*, *16*(10), p.106005.

113. Nguyen, T., Babawale, O., Kim, T., Jo, H.J., Liu, H. and Kim, J.G., 2018. Exploring brain functional connectivity in rest and sleep states: a fNIRS study. *Scientific reports*, *8*(1), p.16144

114. Sämann, P.G., Wehrle, R., Hoehn, D., Spoormaker, V.I., Peters, H., Tully, C., Holsboer, F. and Czisch, M., 2011. Development of the brain's default mode network from wakefulness to slow wave sleep. *Cerebral cortex*, *21*(9), pp.2082-2093.

115. Horovitz, S.G., Braun, A.R., Carr, W.S., Picchioni, D., Balkin, T.J., Fukunaga, M. and Duyn, J.H., 2009. Decoupling of the brain's default mode network during deep sleep. *Proceedings of the National Academy of Sciences*, *106*(27), pp.11376-11381.

116. Igawa, M., Atsumi, Y., Takahashi, K., Shiotsuka, S., Hirasawa, H., Yamamoto, R., Maki, A., Yamashita, Y. and Koizumi, H., 2001. Activation of visual cortex in REM

sleep measured by 24-channel NIRS imaging. *Psychiatry and clinical neurosciences*, *55*(3), pp.187-188

117. Kubota, Y., Takasu, N.N., Horita, S., Kondo, M., Shimizu, M., Okada, T., Wakamura, T. and Toichi, M., 2011. Dorsolateral prefrontal cortical oxygenation during REM sleep in humans. *Brain research*, *1389*, pp.83-92.

118. Candès, E.J., 2006, August. Compressive sampling. In *Proceedings of the international congress of mathematicians*, 3, pp. 1433-1452.

Appendix

Sleep statistics

The timings of each subject in different stages of their sleep during the whole night varied considerably from one another as shown in the table below. The times are shown in minutes.

	Subject1	**Subject 2**	**Subject 3**	**Subject 4**	**Subject 5**
Wake	36.0	75.0	16.5	13.0	7.0
NREM1	23.5	25.0	37.0	25.5	16.5
NREM2	145.5	280.5	170.0	214.0	207.5
NREM3	43.0	28.0	68.0	128.5	166.0
REM	37.5	97.0	39.5	77.0	390.0